PROF. MIGUEL A. VALVANO (Orcid ID : 0000-0001-8229-3641)

PROF. LOTTE SØGAARD-ANDERSEN (Orcid ID : 0000-0002-0674-0013)

Article type : Research Article

# Identification of the Wzx flippase, Wzy polymerase and sugar-modifying enzymes for spore coat polysaccharide biosynthesis in *Myxococcus xanthus*

María Pérez-Burgos[1], Inmaculada García-Romero[2], Miguel A. Valvano[2], and Lotte Søgaard-Andersen[1]*

[1] Max Planck Institute for Terrestrial Microbiology

Department of Ecophysiology

Karl-von-Frisch Str. 10

35043 Marburg, Germany

[2] Wellcome-Wolfson Institute for Experimental Medicine

Queen's University Belfast

Belfast, BT9 7BL, United Kingdom

This article has been accepted for publication and undergone full peer review but has not been through the copyediting, typesetting, pagination and proofreading process, which may lead to differences between this version and the Version of Record. Please cite this article as doi: 10.1111/MMI.14486

Running title: Spore coat polysaccharide biosynthesis in *M. xanthus*

* Corresponding author

Tel. +49-6421-178 201

Fax +49-6421-178 209

E-mail: sogaard@mpi-marburg.mpg.de

**Summary**

The rod-shaped cells of *Myxococcus xanthus,* a Gram-negative deltaproteobacterium, differentiate to environmentally resistant spores upon starvation or chemical stress. The environmental resistance depends on a spore coat polysaccharide that is synthesized by the ExoA-I proteins, some of which are part of a Wzx/Wzy-dependent pathway for polysaccharide synthesis and export; however, key components of this pathway have remained unidentified. Here, we identify and characterize two additional loci encoding proteins with homology to enzymes involved in polysaccharide synthesis and export, as well as sugar modification, and show that six of the proteins encoded by these loci are essential for the formation of environmentally resistant spores. Our data support that MXAN_3260, renamed ExoM, and MXAN_3026, renamed ExoJ, are the Wzx flippase and Wzy polymerase, respectively responsible for translocation and polymerization of the repeat unit of the spore coat polysaccharide. Moreover, we provide evidence that three glycosyltransferases (MXAN_3027/ExoK, MXAN_3262/ExoO and MXAN_3263/ExoP) and a polysaccharide deacetylase (MXAN_3259/ExoL) are important for formation of the intact spore coat, while ExoE is the polyisoprenyl-phosphate hexose-1-phosphate transferase responsible for initiating repeat unit synthesis, likely by transferring *N*-acetylgalactosamine-1-P to undecaprenyl-phosphate. Together, our data generate a more complete model of the Exo pathway for spore coat polysaccharide biosynthesis and export.

**Abbreviated Summary**

*Myxococcus xanthus* differentiates to environmentally resistant spores in response to various stresses. Resistance is provided by the spore coat polysaccharide that is synthesized by the ExoA-I proteins, which make up an incomplete Wzx/Wzy pathway for polysaccharide synthesis and export. Here, we identified the Wzx flippase and Wzy polymerase as well as three glycosyltransferase and a polysaccharide deacetylase that are important for formation of the intact spore coat, thus, providing a more complete Exo pathway.

Keywords: Development, Exo, Nfs, polysaccharide, O-antigen, sporulation

**Introduction**

Bacteria have evolved different strategies that enable their survival in response to environmental changes. Often these strategies include alterations in gene expression, motility behaviour and/or metabolism without evident changes in cell morphology. However, as an alternative strategy, some bacteria undergo cellular differentiation resulting in the formation of cell types with altered morphology and novel characteristics. The best-studied examples of environmentally induced bacterial differentiation include spore formation in three phylogenetically widely separated species *Bacillus subtilis* (Tan & Ramamurthi, 2014), *Streptomyces coelicolor* (Flärdh & Buttner, 2009), and *Myxococcus xanthus* (Konovalova *et al.*, 2010). While the spore formation process varies among these three species, the resulting spores have in common that they have a spore coat that confers resistance to environmental stress.

In *B. subtilis*, sporulation is initiated in response to starvation and depends on an unusual cell division event in which the division septum is placed asymmetrically close to a cell pole, resulting in the formation of a large mother cell and a smaller forespore. Next, the mother cell engulfs the forespore and lysis of the mother cell finally releases the mature spore (Tan & Ramamurthi, 2014). The spore envelope, partly generated by the mother cell and partly by the forespore, consists of a multilayered structure comprising from inside to outside: the cytoplasmic membrane, peptidoglycan (PG), an outer membrane, which is originally the cytoplasmic membrane of the mother cell, and a proteinaceous coat (McKenney *et al.*, 2013, Driks & Eichenberger, 2016). In response to nutrient depletion, *S. coelicolor* generate aerial hyphae and, here, multiple synchronous cell divisions give rise to the spores (Flärdh & Buttner, 2009, Sigle *et al.*, 2015). The spore envelope of *S. coelicolor* is less well-studied but contains PG, a proteinaceous sheath made of chaplins and rodlins, and spore wall teichoic acids (Flärdh & Buttner, 2009, Sigle *et al.*, 2015). In the Gram-negative deltaproteobacterium *M. xanthus*, sporulation is also typically induced by starvation (Konovalova *et al.*, 2010). However, in this bacterium, spores are formed independently of a cell division event, and during the sporulation process, PG is replaced by a spore coat consisting mainly of polysaccharide. Here, we focus on the identification of proteins important for formation of the spore coat polysaccharide in *M. xanthus*.

In response to nutrient limitation, the rod-shaped cells of *M. xanthus* initiate a developmental program resulting in the formation of multicellular spore-filled fruiting bodies (Konovalova *et al.*, 2010). Fruiting bodies are formed as cells aggregate to form mounds during the first 24 h of starvation. These mounds eventually convert into fruiting bodies as the rod-shaped cells that have accumulated inside the mounds begin to differentiate into spherical desiccation-, heat- and sonication resistant spores. Spore morphogenesis occurs from ~24 h and over the next 48 h; in

this process, the ~7 μm × ~0.5 μm rod-shaped cells are remodelled to become shorter and wider, ultimately forming spherical spores with a diameter of 1-2 μm (Dworkin & Voelz, 1962, Dworkin & Gibson, 1964). The PG cell wall is removed during this cellular remodelling process; in parallel, the spore coat is synthesized (Bui *et al.*, 2009, Holkenbrink *et al.*, 2014, Müller *et al.*, 2012). The spore coat consists of a thick layer of polysaccharide and several proteins outside of the outer membrane (OM) (McCleary *et al.*, 1991, Inouye *et al.*, 1979a, Leng *et al.*, 2011). While none of these proteins are essential for spore formation (Komano *et al.*, 1984, Inouye *et al.*, 1979b, Leng *et al.*, 2011, Lee *et al.*, 2011, Curtis *et al.*, 2007), lack of the spore coat polysaccharide causes a sporulation defect (Holkenbrink *et al.*, 2014, Müller *et al.*, 2012). Because only cells inside fruiting bodies differentiate to spores, starvation-dependent sporulation depends on the processes that are important for aggregation of cells into mounds including intra- and intercellular signalling cascades, exopolysaccharide (EPS), lipopolysaccharide (LPS) and motility (Konovalova *et al.*, 2010). Interestingly, spore formation can also occur independently of starvation, i.e. in the presence of nutrients, in response to addition of glycerol (Dworkin & Gibson, 1964), other alcohols (e.g. isopropanol and ethylene glycol) (Sadler & Dworkin, 1966), dimethyl sulfoxide (Komano *et al.*, 1980), or β-lactams and D-amino acids (O'Connor & Zusman, 1997). Spore formation by this process, often referred to as chemically-induced sporulation, occurs rapidly and synchronously within 4-8 h; these spores are not identical to the spores formed in response to starvation since the spore coat polysaccharide is thinner and several proteins that are present in starvation-induced spores are absent (Inouye *et al.*, 1979a, Inouye *et al.*, 1979b, McCleary *et al.*, 1991, Müller *et al.*, 2012, Otani *et al.*, 1998, Downard & Zusman, 1985, Komano *et al.*, 1980). However, the morphogenesis process associated with chemically-induced sporulation involves a similar cellular remodelling process as for starvation-induced spores; the composition of the spore coat polysaccharide appears to be similar in both (Kottel *et al.*, 1975, Sutherland & Mackenzie, 1977) and formation of the spore coat polysaccharide is essential for formation of both types of spores (Licking *et al.*, 2000, Müller *et al.*, 2012).

Synthesis of the *M. xanthus* spore coat polysaccharide involves the ExoA-I proteins and the NfsA-H/AglQRS systems (Holkenbrink *et al.*, 2014, Ueki & Inouye, 2005, Müller *et al.*, 2012, Licking *et al.*, 2000, Wartel *et al.*, 2013). The ExoA-I proteins, encoded by the *exoA-I* locus, were suggested to be components of an incomplete Wzx/Wzy-dependent pathway for polysaccharide synthesis and export (Table S1 and Fig. 1A) (Valvano, 2011, Valvano *et al.*, 2011, Schmid *et al.*, 2015, Holkenbrink *et al.*, 2014, Müller *et al.*, 2012). The NfsA-H machinery, encoded by the *nfsA-H* locus, localize to the cell envelope (Holkenbrink *et al.*, 2014) and is thought to be powered by the AglQRS proteins in a proton motive force-dependent manner (Wartel *et al.*, 2013).. While

these proteins are important for sporulation, they are not required for spore coat polysaccharide synthesis and export but rather function to modify the ExoA-I-produced polysaccharide to generate the rigid, stress-bearing spore coat (Holkenbrink *et al.*, 2014, Müller *et al.*, 2012, Wartel *et al.*, 2013). This modification involves an alteration in spore coat polysaccharide chain length by an unknown mechanism (Holkenbrink *et al.*, 2014).

In Wzx/Wzy pathways, the individual repeat units of the polysaccharide chain are synthesized in the cytoplasm on the lipid carrier undecaprenyl-phosphate (Und-P) in a process that is primed by a polyisoprenyl-phosphate hexose-1-phosphate transferase (PHPT) or a polyisoprenyl-phosphate *N*-acetylhexosamine-1-phosphate transferase (PNPT). Next, specific glycosyltransferases (GTs) transfer the additional sugar building blocks from nucleotide-sugar donors to the Und-PP-sugar primer molecule to generate the Und-PP-repeat unit, which can be further modified by additional enzymes. Individual repeat units are transported across the inner membrane (IM) by the Wzx flippase, assembled into the polysaccharide by the Wzy polymerase together with a polysaccharide co-polymerase (PCP) protein, and transported across the OM by a Wza OM polysaccharide export (OPX) protein (Valvano *et al.*, 2011). In the Exo pathway (Fig. 1A), ExoE is a predicted PHPT responsible for priming synthesis of individual repeat units (Holkenbrink *et al.*, 2014). The integral membrane protein ExoC together with the cytoplasmic ExoD tyrosine kinase form part of a bipartite Wzc protein of the PCP-2 family, in which ExoD (formerly BtkA (Kimura *et al.*, 2011)) is thought to participate in regulating ExoC activity (Kimura *et al.*, 2011, Holkenbrink *et al.*, 2014). ExoA (formerly FdgA (Ueki & Inouye, 2005)) is a homolog of Wza OPX proteins (Holkenbrink *et al.*, 2014). ExoG and ExoI are *N*-acetyltransferase homologs that could be involved in modifying sugars before or after incorporation into the Und-PP-repeat units before export; ExoH is homologous to aminotransferases, ExoF is a putative gluconeogenesis factor, and ExoB is an OM β-barrel protein of unknown function (Holkenbrink *et al.*, 2014). All Exo proteins except for ExoF are essential for sporulation and synthesis of an intact spore coat polysaccharide (Holkenbrink *et al.*, 2014, Ueki & Inouye, 2005, Licking *et al.*, 2000). Generally, Wzc proteins of the PCP-2 family are components of Wzx/Wzy dependent pathways for polysaccharide synthesis and export (Morona *et al.*, 2009) supporting the notion that the ExoA-I proteins are part of a Wzx/Wzy pathway. Notably, such an Exo pathway is incomplete and lacks several key enzymes including the GTs that add sugars from nucleotide-sugar donors to the Und-PP-sugar primer molecule, the Wzx flippase and the Wzy polymerase (Fig. 1A).

Here, we report the identification of two additional gene clusters encoding seven proteins that have homology to enzymes involved in polysaccharide synthesis and/or modification and show that they are essential for sporulation and by implication for synthesis of the spore coat

polysaccharide. We identify MXAN_3260 as the Wzx flippase (renamed ExoM) and MXAN_3026 (renamed to ExoJ) as the Wzy polymerase. We also identify five additional proteins important for spore coat polysaccharide synthesis including three GTs, and determine the nucleotide sugar specificity of the ExoE priming enzyme, thus, generating a more complete model of the Exo pathway for spore coat polysaccharide biosynthesis.

**Results**

Identification of two loci encoding a Wzx flippase, a Wzy polymerase and other proteins involved in polysaccharide synthesis

To identify missing components for spore coat polysaccharide biosynthesis, we used a two-pronged strategy. First, as polysaccharide biosynthesis genes are often clustered (Rehm, 2010), we searched for homologs of the missing components in the *M. xanthus* genome. Because the genome encodes at least 66 GTs, we specifically searched for Wzx flippase and Wzy polymerase homologs (*see Experimental Procedures*). A domain search suggested that the *M. xanthus* genome encodes three Wzx flippase homologs (MXAN_1035, MXAN_3260 and MXAN_7416) and four Wzy_C domain proteins (MXAN_1052, MXAN_2919, MXAN_3026 and MXAN_7442). Second, because expression of the *exoA-I* and *nfsA-H* genes is induced in response to starvation and chemical induction of sporulation (Kimura *et al.*, 2011, Licking *et al.*, 2000, Ueki & Inouye, 2005, Müller *et al.*, 2010, Giglio *et al.*, 2015, Wartel *et al.*, 2013), we identified those candidate genes whose transcription pattern was similar to that of the *exoA-I* and *nfsA-H* genes during chemically-induced sporulation using published data (Müller *et al.*, 2010). Among the seven candidate genes, only the genes for the Wzx homolog MXAN_3260 and the Wzy_C domain protein MXAN_3026 were upregulated (Fig. 1B) suggesting these two proteins could be the missing Wzx flippase and Wzy polymerase, respectively, for spore coat polysaccharide synthesis. Further, mutation of *MXAN_1035* was previously reported to only slightly affect spore formation (Holkenbrink *et al.*, 2014), while *MXAN_1052* is in the same polysaccharide biosynthesis gene cluster as *MXAN_1035* and, therefore, likely also not involved in spore coat synthesis. *MXAN_7416* and *MXAN_7442* are part of the *eps* locus, which is important for EPS synthesis (Lu *et al.*, 2005). Finally, MXAN_2919 is the WaaL O-antigen ligase involved in LPS synthesis (Pérez-Burgos *et al.*, 2019). Therefore, we investigated the Wzx flippase homolog MXAN_3260 and the Wzy polymerase homolog MXAN_3026 for a potential role in spore coat polysaccharide synthesis.

Sequences of Wzx flippases and Wzy polymerases are not well conserved, but both are membrane proteins with a high number of transmembrane helices (TMHs) (Raetz & Whitfield, 2002, Hug & Feldman, 2011). Sequence analysis of MXAN_3260 revealed a PF13440 (Polysacc_synt_3) domain (Fig. 1C), similar to the LPS O-antigen Wzx flippase of *Yersinia similis* serotype O:9 (Beczała *et al.*, 2015), and a PF14667 (Polysacc_synt_C) domain. The protein had also 11 or 12 predicted TMHs according to TMHMM and SPOCTOPUS, respectively (Fig. 1C), as found in other flippases (Valvano, 2011). The Wzy polymerase candidate MXAN_3026 contains a PF04932 (Wzy_C) domain (Fig. 1C), which is also found in O-antigen ligases, Wzy polymerases

and O-linked oligosaccharyltransferases (Schild *et al.*, 2005, Hug & Feldman, 2011), and multiple TMHs whose topology depended on the prediction program used (Fig. 1C).

MXAN_3260 and MXAN_3026 are encoded by genes in two distinct gene clusters that we renamed to *exo* gene cluster III and II, while we renamed the *exoA-I* gene cluster to Exo gene cluster I (Fig. 1D). Analysis of the genetic neighbourhood of *MXAN_3260* and *MXAN_3026* (Fig. 1D; Table S1) showed that MXAN_3262, MXAN_3263 and MXAN_3027 are putative GTs, each containing a single GT4 domain according to the CAZy database. MXAN_3259 is a polysaccharide deacetylase homolog while MXAN_3261 is a serine O-acetyltransferase homolog. In the three *exo* gene clusters, all genes for which published microarray data are available are up-regulated during chemically-induced sporulation with 0.5 M glycerol (Fig. 1E) (Müller *et al.*, 2010). As discussed in details below, *exo* gene cluster I and III make up one cluster in *Vulgatibacter incomptus* and all three clusters are present as one cluster in Anaeromyxobacteraceae supporting that the gene products of the three clusters may function together.

As shown below, the genes of *exo* gene cluster II and III are important for sporulation and our data support that the encoded proteins form part of the same machinery. For simplicity and to facilitate identification of the genes throughout this study, we renamed MXAN_3026, MXAN_3027 and MXAN_3259-MXAN_3263 to ExoJ-P following the Exo nomenclature (Holkenbrink *et al.*, 2014, Müller *et al.*, 2012) (Fig. 1D).

ExoJ-ExoP are important for chemically-induced sporulation

To determine the importance of the seven *exoJ-P* genes in sporulation, we generated in-frame deletion mutations in each of the genes separately and determined their importance for sporulation using chemical induction (Fig. 2AB). After addition of glycerol to a final concentration of 0.5 M, wild-type (WT) cells rounded up during the first 4 h and had turned into phase-bright resistant spores by 24 h. Cells of the Δ*exoE* mutant, which cannot produce spore coat polysaccharide (Holkenbrink *et al.*, 2014), served as a negative control. As previously described (Holkenbrink *et al.*, 2014), Δ*exoE* cells initially shortened becoming ovoid by 4 h; by 24 h, most Δ*exoE* cells had reverted to a non-phase bright rod-shape while a few remained non-phase-bright ovoid-shaped or were branched and non-phase-bright. Δ*exoE* cells were not resistant to heat and sonic treatment.

The Δ*exoM* and Δ*exoJ* mutants formed large round cells by 4 h; by 24 h, many cells had reverted to rod-shape, however, a significant fraction were ovoid, branched or formed large spheres; cells of these two mutants were neither phase-bright nor resistant to heat and sonic treatment. The

Δ*exoK,* Δ*exoO* and Δ*exoP* mutants had cell morphologies and sporulation defects similar to those of the Δ*exoM* and Δ*exoJ* mutants. By 4 h, Δ*exoL* cells were ovoid; by 24 h, many of these cells had reverted to rod-shape, however, a significant fraction were ovoid and a few were branched or had turned into large spheres. None of these cells were phase bright or resistant to heat and sonic treatment. Finally, the Δ*exoN* mutant formed phase-bright spores that were resistant to heat and sonic treatment but at a two-fold reduced level compared to WT; moreover, a significant fraction of cells at 24 h were non-phase bright rod-shaped or ovoid while a small fraction were branched or formed large spheres. Sporulation of all eight in-frame deletion mutants was restored by ectopic expression of the corresponding full-length gene under the control of the native promoter ($P_{nat}$) on a plasmid integrated in a single copy at the Mx8 *attB* site (Fig. 1D; Fig. 2).

We conclude that all seven ExoJ-P proteins, except ExoN, are essential for chemically-induced sporulation. These data agree with the idea that ExoM is the Wzx flippase, ExoJ the Wzy polymerase, ExoK/-O/-P GTs and ExoL a polysaccharide deacetylase essential for synthesis of an intact spore coat polysaccharide, and are also consistent with a previous report that an insertional mutation in *exoJ* caused a sporulation defect (Müller *et al.*, 2012). Of note, cells lacking ExoE, which are blocked in the initiation of repeat unit synthesis because they lack the PHPT for spore coat polysaccharide synthesis, mostly reverted from ovoid at 4 h to rod-shaped at 24 h while the remaining mutants, which would be impaired in spore coat polysaccharide synthesis at later steps, formed morphologically highly abnormal cells (ovoid-shaped, branched or large spheres) by 24 h (Fig. 2B) (see Discussion).

Loss of ExoE and ExoJ-ExoP neither affects EPS and LPS synthesis, cell morphology nor motility

In addition to the spore coat polysaccharide, *M. xanthus* synthesizes two additional polysaccharides, i.e. EPS and LPS, both of which are important for fruiting body formation. Because blocking synthesis of one glycan polymer can affect synthesis of other polymers including PG by sequestration of Und-P through accumulation of Und-PP intermediates (Valvano, 2008, Burrows & Lam, 1999, Jorgenson & Young, 2016, Jorgenson *et al.*, 2016, Ranjit & Young, 2016), we determined whether lack of Exo proteins interferes with EPS, LPS or PG synthesis during growth.

EPS synthesis was tested using nutrient-rich agar supplemented with Congo red. As a result of binding of the dye to EPS, WT colonies acquired a red colour while the negative control, a Ω*difE* mutant (Yang *et al.*, 1998), did not (Fig. 3A). All *exo* mutants tested accumulated EPS at WT level. LPS was extracted from cell extracts from growing cells and detected by Emerald green

staining. For WT as well as all tested *exo* mutants, a fast running lipid-A core band and polymeric LPS O-antigen bands were detected while only the lipid-A core band was detected in the Δ*wbaP* negative control strain, which is impaired in O-antigen synthesis (Pérez-Burgos *et al.*, 2019) (Fig. 3B). Because interference with PG synthesis causes the formation of abnormally shaped cells including filamentous cells in the presence of nutrients (Treuner-Lange *et al.*, 2015, Treuner-Lange *et al.*, 2013, Schumacher *et al.*, 2017), we used cell morphology as a proxy for PG synthesis to test whether lack of the Exo proteins interferes with PG synthesis during growth. Lack of the tested components of the Exo machinery did not affect cell morphology (Fig. 2 (0 h) and 3C), with the exception of Δ*exoL* cells, which were marginally but significantly (p=0.029) shorter than WT. Therefore, loss of spore coat polysaccharide synthesis does not interfere with EPS, LPS or PG synthesis during growth in agreement with the observation that *exo* gene expression is induced during sporulation. Moreover, these observations support that the Exo machinery is dedicated to spore coat synthesis and that the EPS, LPS and PG machineries function independently of the Exo proteins during growth.

*M. xanthus* possesses two distinct motility systems that are important for fruiting body formation; one of them depends on type IV pili (T4P) and the other one depends on the Agl/Glt gliding motility complexes (Schumacher & Søgaard-Andersen, 2017, Zhang *et al.*, 2012). EPS and LPS are important for motility (Lu *et al.*, 2005, Pérez-Burgos *et al.*, 2019). On 0.5 % agar, which favours T4P-dependent motility, WT displayed the flares characteristic of this type of motility; by contrast, the negative control Δ*pilA* strain, which lacks the major pilin of T4P (Wu & Kaiser, 1996), did not. On 1.5 % agar, which favours gliding motility, single cells were observed at the colony edge of WT, while the Δ*aglQ* mutant, which lacks an essential component of the gliding machinery motor (Nan *et al.*, 2013, Sun *et al.*, 2011), had a smooth edge. By contrast, all tested *exo* mutants were indistinguishable from WT (Fig. S1; Table 1). Together, these results indicate that loss of the Exo machinery does not interfere with motility during growth.

ExoJ-M and ExoO-P are important for starvation-induced sporulation

Having shown that the Exo proteins are neither important for EPS, LPS or PG biosynthesis nor for motility during growth, we asked whether the *exo* mutants are able to generate starvation-induced spores during fruiting body formation. Previous analyses showed that Δ*exoA,* Ω*exoC*, Δ*exoC*, Ω*exoD* and Ω*exoJ* mutants are generally able to form fruiting bodies but have a reduced sporulation efficiency (Licking *et al.*, 2000, Müller *et al.*, 2012, Ueki & Inouye, 2005, Kimura *et al.*, 2011). Because these experiments were performed under different conditions, we tested the

developmental proficiency of eight *exo* mutants on TPM 1.5% agar and under submerged conditions.

Similar to WT, all eight *exo* mutants had aggregated to form fruiting bodies by 24 h under both conditions (Fig. S2). However, all *exo* mutants with the exception of the Δ*exoN* mutant had a strong sporulation defect (Fig. S2; Table 1). Importantly, the sporulation defects were partially or completely complemented by ectopic expression of the relevant full-length gene from the native promoter (Fig. 1D; S2; Table 1). Because the sporulation defects of the *exo* mutants during chemically-induced sporulation were fully complemented, we speculate that the partial complementation observed for some of the *exo* mutants is caused by insufficient expression of the relevant gene during starvation. As in the case of chemically-induced sporulation, we conclude that ExoJ-P proteins, with the exception of ExoN, are essential for starvation-induced sporulation and by implication in formation of an intact spore coat.

ExoE has GalNAc-1-P transferase activity

ExoE was suggested to be the PHPT homolog that initiates repeat unit biosynthesis for spore coat polysaccharide biosynthesis (Holkenbrink *et al.*, 2014); however, it is unknown which sugar ExoE transfers to Und-P. Similarly to the *Escherichia coli* $WcaJ_{Ec}$, which transfers Glc-1-P to Und-P, and the *Salmonella enterica* $WbaP_{Se}$, which transfers Gal-1-P to Und-P (Saldías *et al.*, 2008, Furlong *et al.*, 2015), ExoE contains a PF02397 (Bacterial Sugar Transferase) domain in the C-terminus and five putative transmembrane domains (Fig. 4A). By contrast, PNPTs including the *E. coli* $WecA_{Ec}$, which transfers GlcNAc-1-P to Und-P, contain a PF00953 (Glycosyl transferase family 4) domain (Fig. 4A) (Lehrman, 1994). In $WcaJ_{Ec}$, the fifth TMH forms a helix-break-helix structure and does not fully span the IM resulting in the cytoplasmic localization of the C-terminal catalytic domain. This depends on the residue P291 that forms part of a $DX_{12}P$ motif highly conserved among PHPTs (Furlong *et al.*, 2015). ExoE also carries the $DX_{12}P$ motif and contains all the other conserved essential residues important for catalytic activity that have been identified in the C-terminal catalytic domain of $WbaP_{Se}$ (Patel *et al.*, 2010) (Fig. 4B and Fig. S3). Thus, ExoE is a PHPT with a predicted topology similar to that described for $WcaJ_{Ec}$ and $WbaP_{Se}$.

Compositional analysis of the spore coat polysaccharide showed that it is composed of 1-3-, 1-4-linked GalNAc, 1-4-linked Glc (GalNAc:Glc ratio 17:1) and glycine (Holkenbrink *et al.*, 2014). These findings suggest that ExoE could use either UDP-Glc or UDP-GalNAc as a substrate. To test the activity of ExoE, we performed heterologous expression experiments in *E. coli* and *S. enterica*. To this end, we generated the plasmids pMP158 and pMP147, which encode native,

untagged ExoE and a FLAG-tagged ExoE variant ($_{FLAG}$ExoE), respectively from an arabinose-inducible promoter in plasmid pBAD24. We used native ExoE to test for ExoE activity and $_{FLAG}$ExoE to test for protein accumulation using immunoblotting.

To determine whether ExoE can use UDP-Glc, we carried out heterologous complementation experiments in a Δ*wcaJ*$_{Ec}$ *E. coli* strain, which lacks the ability to produce colanic acid as previously reported (Patel *et al.*, 2012, Pérez-Burgos *et al.*, 2019). For this experiment, native ExoE was synthesized in the Δ*wcaJ*$_{Ec}$ strain also containing pWQ499, which encodes the RcsA regulator that increases the production of colanic acid (Furlong *et al.*, 2015). Cells growing in the absence and presence of arabinose were examined for a glossy and mucoid colony phenotype characteristic of colanic acid capsule production (Fig. 4C). Only cells containing the $_{FLAG}$WcaJ$_{Ec}$-encoding plasmid pLA3 exhibited the distinct mucoid phenotype representing colanic acid production, whereas the strain synthesizing native ExoE or containing the pBAD24 vector control did not display this phenotype. As shown in Fig. S4A, $_{FLAG}$ExoE accumulated although at a slightly lower level than $_{FLAG}$WcaJ$_{Ec}$. Together, these results indicate ExoE is not a Glc-1-P transferase.

PHPT proteins were initially described as hexose-1-phosphate transferases while PNPTs are considered *N*-acetylhexosamine-1-phosphate transferases; however, there are several examples of proteins of the PHPT family with specificities for *N*-acetylated nucleotide sugars (Glover *et al.*, 2006, Power *et al.*, 2000, Merino *et al.*, 2011, Chamot-Rooke *et al.*, 2007). Because ExoE did not transfer Glc-1-P, we next investigated whether ExoE could transfer GalNAc-1-P. To this end, we performed heterologous expression experiments in *E. coli* in which we first tested for transfer of GlcNAc-1-P and subsequently for transfer of GalNAc-1-P. GlcNAc-1-P transferase activity can be tested using the *E. coli* strain MV501, which has a transposon insertion in *wecA*$_{Ec}$. As described, WecA$_{Ec}$ is a PNPT that uses UDP-GlcNAc for initiating synthesis of O7 polysaccharide antigen (Alexander & Valvano, 1994). Native ExoE in MV501 did not restore O7 polysaccharide synthesis (Fig. 4D). In immunoblot experiments we observed that $_{FLAG}$ExoE accumulated in MV501, especially in an oligomeric form, although at a low level (Fig. S4B). By contrast, pMAV11 carrying the *wecA*$_{Ec}$ gene complemented the defect in O-antigen synthesis. These observations suggest that ExoE is not a GlcNAc-1-P transferase.

*E. coli* lacks the Gne epimerase, which interconverts UDP-GlcNAc and UDP-GalNAc. Previously, Merino et al. (Merino *et al.*, 2011) demonstrated that the *Aeromonas hydrophila* PHPT homolog WecP$_{Ah}$ in the presence of a plasmid encoding the Gne homolog from *A. hydrophila* modified the MV501 lipid A-core. This modification is consistent with formation of an O7 repeat containing GalNAc. This modified lipid A-core likely only contains one O7 repeat because the addition of

GalNAc to the repeat may interfere with O7 polymerization (Merino *et al.*, 2011). Similar to Merino et al., we observed formation of this GalNAc containing O7 repeat in MV501 in the presence of plasmids encoding $_{FLAG}WecP_{Ah}$ (pSEF88) and the *A. hydrophila* Gne homolog (pGEMT-$Gne_{Ah}$) (Fig. 4E). More importantly, co-expression of ExoE and $Gne_{Ah}$ in MV501 resulted in a lipid A-core modified band similar to that observed with co-expression of $_{FLAG}WecP_{Ah}$ and $Gne_{Ah}$ (Fig. 4E). This result supports that ExoE can transfer GalNAc-1-P to Und-P in *E. coli.*

Finally, we investigated the specificity of ExoE for UDP-Gal, in this case using the *S. enterica* Δ*wbaP*$_{Se}$ mutant MSS2 that is blocked in the first step in O-antigen synthesis. ExoE did not restore O-antigen synthesis in MSS2 despite the FLAG-tagged variant of the protein accumulating (Fig. 4F-G and Fig. S4A). By contrast, the control plasmids pJD132 and pSM13, which encode $WbaP_{Ec\ O9:K30}$ of *E. coli* and $WbaP_{Se}$ of *S. enterica*, respectively, both restored O-antigen synthesis (Fig. 4F-G). Collectively, the heterologous expression experiments support that ExoE has specificity for UDP-GalNAc but lacks specificity for UDP-Glc, UDP-GlcNAc, and UDP-Gal. These data, together with the observation that the spore coat polysaccharide contains Glc and GalNAc suggest that ExoE is a GalNAc-1-P transferase forming Und-PP-GalNAc and that GalNAc is likely the first sugar added to Und-P during the biosynthesis of the spore coat polysaccharide repeat.

## The *exo* and *nfs* gene clusters co-occur only in a subset of sporulating Myxococcales

Because the majority of the members of the order Myxococcales can sporulate (Reichenbach, 1999), we hypothesized that the Exo and Nfs machineries for formation of the rigid spore coat would be conserved in Myxoccocales. We therefore searched for orthologs of each Exo and Nfs protein in Myxococcales with fully sequenced genomes using a reciprocal best BlastP hit method (Experimental Procedures).

Within the suborder Cystobacterineae, all individual components of the Exo machinery are conserved in F. Myxococcaceae, F. Archangiaceae and F. Vulgatibacteraceae, while there is somewhat less conservation, especially of cluster III, in the Anaeromyxobacteraceae (Fig. 5A). By contrast, in the suborders Nannocystineae and Sorangineae, Exo orthologs were largely missing. Interestingly, in the small genomes of *V. incomptus* and Anaeromyxobacteraceae, that only have approximately half the size of other myxobacterial genomes (Fig. 5A, right), *exo* gene cluster I and III are organized in one cluster (*V. incomptus*), while all three clusters are present in one in Anaeromyxobacteraceae (Fig. 5A; Fig. S5A), lending further support to the idea that these proteins function in the same pathway. The taxonomic distribution of the *exo* genes supports an

evolutionary scenario in which the last common ancestor of the Cystobacterineae acquired the *exo* gene cluster, and then over time gene organization diversified. Alternatively, a common ancestor of the myxobacteria contained the *exo* gene cluster and the *exo* genes were lost in ancestors of the Nannocystineae or Sorangineae.

The NfsA-H proteins are paralogs of the GltA-H proteins that are important for gliding motility (Wartel *et al.*, 2013, Agrebi *et al.*, 2015). While NfsA-H are encoded in one gene cluster, GltA-H are encoded in two gene clusters in the *M. xanthus* genome (Fig. 5AB). In agreement with previous analyses (Agrebi *et al.*, 2015, Luciano *et al.*, 2011) in which conservation of GltA-H/NfsA-H homologs were studied without distinguishing between the two machineries, orthologs of the GltA-H proteins are widely conserved in Myxococcales although with less conservation in the Nannocystineae and Sorangineae. Moreover, the two *glt* gene clusters are in close proximity outside of the F. Myxococcaceae, F. Archangiaceae and F. Vulgatibacteraceae (Fig. 5A; Fig. S5B) as previously described for *Anaeromyxobacter* (Luciano *et al.*, 2011). By contrast, our analysis shows that orthologs of NfsA-H are exclusively found in the F. Myxococcaceae, F. Archangiaceae and F. Vulgatibacteraceae. The taxonomic distribution of the *glt* and *nfs* gene clusters suggests that the primitive *gltA-H* genes were present in the last common ancestor of the Myxococcales and that the *nfs* cluster results from a duplication event of the ancestral *gltA-H* gene cluster shortly after the divergence of the Anaeromyxobacteraceae from the remaining Cystobacterineae. This agrees with a previous suggestion (Agrebi *et al.*, 2015, Luciano *et al.*, 2011), except that our analysis clearly supports that the primitive Glt proteins are ancestral to the Nfs proteins.

Also, our analysis shows that the *exo* and *nfs* genes co-occur in the Cystobacterineae except in the Anaeromyxobacteraceae. Interestingly, except for *V. incomptus,* for which no fruiting body formation and sporulation were observed (Yamamoto *et al.*, 2014), all the species containing both the *exo* and *nfs* gene clusters have been reported to form phase-bright spores. By contrast, *Haliangium ochraceum, Minicystis rosea, Sorangium cellulosum* and *Chondromyces crocatus* also form spores despite they generally lack the Exo and Nfs machineries. These observations suggest that sporulation occurs by a different mechanism in the sporulating Cystobacterineae compared to sporulating Nannocystineae and Sorangineae. Consistently, Sorangineae spores have been reported to be less phase-bright than the *M. xanthus* spores and rod-shaped (Garcia & Müller, 2014b) and *M. rosea* spores are phase-dark and rod-shaped (Garcia *et al.*, 2014).

**Discussion**

Cells of *M. xanthus* generate at least three different polysaccharidic cell surface structures, namely LPS, EPS and the spore coat polysaccharide. Here, we focused on identifying the proteins that would function together with the ExoA-I proteins in spore coat polysaccharide biosynthesis and export.

Using bioinformatics and gene co-expression analyses, we identified two loci that encode proteins important for sporulation. One of them, named the *exo* gene cluster II, encodes a homolog of Wzy polymerases (ExoJ, MXAN_3026) and a predicted GT (ExoK, MXAN_3027), while the other, *exo* gene cluster III, encodes a predicted polysaccharide deacetylase (ExoL, MXAN_3259), a Wzx flippase (ExoM, MXAN_3260), a serine O-acetyltransferases (ExoN, MXAN_3261) and two GTs (ExoO, MXAN_3262 and ExoP, MXAN_3263). All seven proteins with the exception of ExoN, which is only partially required, are essential for sporulation and, therefore, predicted to function in formation of the intact spore coat polysaccharide. Based on these findings, we propose a revised model for spore coat polysaccharide biosynthesis (Fig. 6).

The *M. xanthus* spore coat polysaccharide is composed of 1-3-, 1-4-linked GalNAc, 1-4-linked Glc and glycine (Holkenbrink *et al.*, 2014) and with the latter proposed to form glycine bridges between polysaccharide chains (Holkenbrink *et al.*, 2014). The spore coat polysaccharide is also acetylated (Holkenbrink *et al.*, 2014, Filer *et al.*, 1977b). However, the precise structure of the spore coat polysaccharide is unknown. The data of Holkenbrink et al. (Holkenbrink *et al.*, 2014), together with our results, suggest a model in which ExoE is the PHPT homolog responsible for the first step in repeat unit synthesis by catalysing the transfer of a sugar-1-P donor to Und-P (Holkenbrink *et al.*, 2014). Here, we demonstrate that ExoE is functionally similar to $WecP_{Ah}$, a GalNAc-1-P transferase from *A. hydrophila* (Merino *et al.*, 2011) in heterologous expression experiments in *E. coli*, suggesting that GalNAc is the first sugar of the spore coat repeat unit. Alternatively, because several of the Exo proteins are sugar modifying enzymes, it is also possible that ExoE has affinity for GalNAc in *E. coli* but incorporates a modified GalNAc as the first sugar in the repeat unit in *M. xanthus*. Subsequently, we predict that the GTs ExoK, ExoO and ExoP transfer sugar building blocks to the repeat unit, which is likely a tetrasaccharide. The *N*-acetyltransferase homologs ExoG and ExoI, the aminotransferase homolog ExoH and the polysaccharide deacetylase homolog ExoL presumably modify sugars before or after incorporation into the repeat unit.

Based on the composition of the spore coat polysaccharide (Holkenbrink *et al.*, 2014), we suggest that the GTs ExoK, ExoO and ExoP incorporate GalNAc and Glc into the repeat unit.

Acetylation of the spore coat polysaccharide may involve the ExoG and ExoI *N*-acetyltransferases (but see also below). ExoL is the first identified potential polysaccharide deacetylase implicated in *M. xanthus* spore coat synthesis. Interestingly, phase bright spores were not detected in the *exoG* and *exoI* mutants (Holkenbrink *et al.*, 2014); similarly, the *exoL* mutant did not form phase bright spores (here) suggesting that proper acetylation of the spore coat polysaccharide is important for its synthesis, stability and/or function. However, it is unknown which residue is modified by ExoG, ExoI and ExoL, and whether these proteins function on the same or independent targets. In *Caulobacter crescentus*, the polysaccharide deacetylase HfsH and the *N*-acetyltransferase HfsK affect acetylation of the holdfast polysaccharide; in the absence of any of these two proteins there is a defect in adhesive and cohesive properties of the holdfast polysaccharide without affecting its synthesis (Wan *et al.*, 2013, Sprecher *et al.*, 2017).

ExoH is predicted to be a pyridoxal phosphate-dependent (PLP) aminotransferase with a DegT/DnrJ/EryC1/StrS family domain (PF01041), which generally catalyses the transfer of an amino group from an amino acid to an amino acceptor (John, 1995). Similarly to the aminotransferase ArnB that transfers an amino group to arabinose in *S. enterica* (Noland *et al.*, 2002) or the PLP aminotransferase PseC from *Helicobacter pylori,* which transfers an amino group to a sugar moiety prior to acetylation by PseH (Ud-Din *et al.*, 2015), we suggest that ExoH may add an amino group to monosaccharides before their incorporation into the repeat unit or modify sugar(s) in the repeat unit.

The glycine in the spore coat polysaccharide was proposed to form glycine bridges between polysaccharide chains (Holkenbrink *et al.*, 2014). Holkenbrink et al. also suggested that glycine is added to the spore coat polysaccharide in the cytoplasm. Interestingly, a structure-based search with HHPred revealed that the closest homolog of the *N*-acetyltransferases ExoG and ExoI is FemX from *Staphylococcus aureus*, i.e. for ExoG and ExoI, the probabilities of homology to FemX is 100% with an E-value of 1.9e-31 and 100% with an E-value of 4.1e-30. The Fem proteins belong to GCN5-related *N*-acetyltransferases (GNAT) that generally transfer acetylated molecules to an amino-acceptor of different target molecules including sugars (Favrot *et al.*, 2016, Ud-Din *et al.*, 2015, Reith & Mayer, 2011). In *S. aureus*, the FemA/B/X proteins add five glycine residues to the lysine in the stem peptide of the lipid II PG precursor using glycyl-charged tRNA molecules as substrates (Favrot *et al.*, 2016). The pentaglycine modification crosslinks PG glycan chains (Favrot *et al.*, 2016). Therefore, it is tempting to speculate that one or both of ExoG and ExoI rather than being involved in acetylation of the spore coat repeat unit could be involved in glycine addition to amino group(s) in the repeat unit. In this context, we speculate that the amino group added by ExoH could serve as an acceptor for glycine transfer. This is also

consistent with the absence of glycine modified sugars after acid hydrolysis of the spore coat polysaccharide (Holkenbrink *et al.*, 2014). Amino acid modified sugars, in this case with serine, have also been identified in the K40 capsular polysaccharide of *E. coli* O8 and the modification demonstrated to be essential for the polymerization of the capsular repeat unit (Amor *et al.*, 1999).

Two Exo proteins are important, but not essential, for formation of phase-bright spores, and by implication spore coat synthesis: ExoF (Holkenbrink *et al.*, 2014) and ExoN (here). ExoN is a putative serine O-acetyltransferase, which are commonly involved in the first step of cysteine synthesis from serine. *M. xanthus* utilizes amino acids and lipids as carbon and energy sources and does not grow on carbohydrates because it lacks required catabolic enzymes (Dworkin, 1962, Hemphill & Zahler, 1968, Watson & Dworkin, 1968). During glycerol-induced sporulation, genes for large portions of the TCA cycle are downregulated, whereas genes for the glyoxylate shunt and gluconeogenesis are upregulated (Müller *et al.*, 2010), e.g. the activity of at least six enzymes putatively involved in synthesis of the major spore coat component UDP-GalNAc increases in response to glycerol addition prior to shortening of cells (Filer *et al.*, 1977a). Given these metabolic changes, we speculate that ExoN may contribute to synthesis of monosaccharides or other metabolites important for spore coat polysaccharide synthesis and, therefore, without ExoN, cells may lack this precursor(s). The *M. xanthus* genome encodes two additional serine O-acetyltransferase homologs (*MXAN_1572* and *MXAN_7449*), which may function redundantly with ExoN and, therefore, the Δ*exoN* mutant is still able to form some phase-bright spores. Similarly, the partially dispensable ExoF, which is a putative gluconeogenesis factor, has been suggested to be important for biosynthesis of activated sugar precursors (Holkenbrink *et al.*, 2014).

After the repeat unit has been synthesized on the cytoplasmic side of the IM, translocation occurs via the Wzx flippase homolog ExoM. In the periplasm, the Wzy polymerase ExoJ elongates the chain with the help/control of the Wzc homolog formed by the integral membrane protein ExoC and the cytoplasmic ExoD tyrosine kinase, which could regulate ExoC activity (Kimura *et al.*, 2011). Subsequently, the polysaccharide chain is transported to the cell surface via the Wza OPX homolog ExoA. The Nfs machinery modifies the Exo-generated polysaccharide by an unknown mechanism to generate shorter polysaccharide chains and the rigid polysaccharide spore coat. How, where and when the Nfs proteins do this is not known.

Disruption of the synthesis of one polysaccharide can have pleiotropic effects on the synthesis of other polysaccharidic molecules. It was previously shown that *M. xanthus* cells lacking the PHPT

WbaP for LPS O-antigen synthesize EPS and spore coat and has a normal cell morphology; similarly, mutants that do not synthesize EPS, synthesize LPS and the spore coat polysaccharide (Holkenbrink *et al.*, 2014, Pérez-Burgos *et al.*, 2019, Lu *et al.*, 2005). Here, we show that during growth mutants that are unable to synthesize the spore coat polysaccharide synthesize WT levels of LPS and EPS, and have a normal cell morphology in the absence of glycerol. Together, these observations suggest the existence of dedicated biosynthesis machineries for LPS, EPS and spore coat polysaccharide synthesis.

A fascinating aspect of the sporulation process in *M. xanthus* is that the PG is degraded during spore morphogenesis (Bui *et al.*, 2009). It has been suggested that the spore coat protects cells from bursting due to intracellular turgor in the absence of PG (Bui *et al.*, 2009, Müller *et al.*, 2012). Therefore, we predict that the removal of PG must be closely coordinated with synthesis of the spore coat polysaccharide. Previous research on chemical induction of sporulation in the *exoA-I* mutants showed that mutant cells initiate the sporulation process with cell shortening and widening. However, at a certain point the sporulation process is aborted and cells regain rod-shape even in the continued presence of glycerol. Of note, after abortion of the sporulation process, many cells display severe morphological defects including branching, formation of spiral-shaped cells and formation of large spherical cells (Holkenbrink *et al.*, 2014, Müller *et al.*, 2012). Here, we observed similar morphological defects in mutants impaired in spore coat polysaccharide synthesis after chemical induction of sporulation. Interestingly, cells lacking the PHPT ExoE have less severe shape defects after 4 and 24 h of glycerol-induction than mutants lacking enzymes suggested to act downstream of the priming step. These observations have two implications. First, we speculate that the abortion of the sporulation process in the *exo* mutants (as opposed to cell lysis due to lack of PG as well as spore coat) is caused by a coupling between spore coat polysaccharide synthesis and the PG removal process. Therefore, in the absence of proper spore coat polysaccharide synthesis, PG would not be completely removed, and cells regain rod-shape through *de novo* synthesis of PG. Because the Exo proteins are not important for PG synthesis during growth, we speculate that the coupling between spore coat polysaccharide synthesis and the PG removal process is regulatory rather than involving shared proteins. Second, we speculate that in the absence of ExoE PHPT activity, Und-P is not sequestered in intermediates for spore coat polysaccharide biosynthesis and, therefore, PG can be resynthesized. By contrast, in the Δ*exoJ-M*, *O-P* mutants (here) and the previously described Δ*exoA-D, G-I* (Holkenbrink *et al.*, 2014) mutants, Und-P would be sequestered in intermediates for spore coat polysaccharide, thus, titrating Und-P away from PG metabolism resulting in more

cells with an abnormal shape. A future goal will be to understand how spore coat polysaccharide synthesis and PG removal is coordinated.

Our analysis of the taxonomic distribution of the *exo* and *nfs* gene clusters lend support to the notion that the spore coat could be synthesized by a different mechanism in sporulating Cystobacterineae compared to sporulating Nannocystineae and Sorangineae. Based on a comparison of gene content in four fruiting body and sporulating Myxococcales (*M. xanthus, Stigmatella aurantiaca, H. ochraceum, S. cellulosum*), we previously reported that key developmental regulators in *M. xanthus* are not widely conserved outside the Cystobacterineae (Huntley *et al.*, 2011). This finding also suggests that the genetic programs for fruiting body formation and sporulation in *M. xanthus* and *S. aurantiaca* are highly similar but significantly different from the genetic program directing fruiting body formation in *S. cellulosum* and *H. ochraceum* (Huntley *et al.*, 2011). The distribution of the *exo* and *nfs* genes supports this scenario also at the level of the spore coat formation. Thus, it remains an open question whether fruiting body formation including sporulation in the Myxococcales is the result of convergent evolution or divergent evolution from a shared primordial genetic program (Huntley *et al.*, 2011).

**Acknowledgement**

The authors thank Jana Jung for constructing SA7455 and SA7489, Sarah Furlong for the gift of pSEF88, Marco Herfurth for the help and discussions with the gene co-occurrence studies and Dobromir Szadkowski for providing the script and guidance with the Matlab analysis. This work was supported by Deutsche Forschungsgemeinschaft (DFG, German Research Council) within the framework of the SFB987 “Microbial Diversity in Environmental Signal Response” as well as by the Max Planck Society.

**Conflict of Interest**

The authors declare no conflict of interest.

**Data Availability**

The data that support the findings of this study are available from the corresponding author upon request.

**Experimental procedures**

Strains and cell growth. *M. xanthus* cells were grown in 1% CTT (1% (w/v) Bacto Casitone, 10 mM Tris-HCl pH 8.0, 1 mM $K_2HPO_4/KH_2PO_4$ pH 7.6 and 8 mM $MgSO_4$) liquid medium or on 1.5% agar supplemented with 1% CTT at 32°C (Hodgkin & Kaiser, 1977). Oxytetracyline and kanamycin were used at final concentrations of 10 μg $ml^{-1}$ and 50 μg $ml^{-1}$, respectively. All *M. xanthus* strains are derivatives of the WT strain DK1622 (Kaiser, 1979). *M. xanthus* strains and plasmids used in this work are listed in Tables 2 and 3, respectively. In-frame deletions were generated as described previously (Shi *et al.*, 2008) and plasmids for complementation experiments were integrated in a single copy by site specific recombination into the Mx8 *attB* site. All in-frame deletions and plasmid integrations were verified by PCR. Plasmids were propagated in *E. coli* Mach1 and DH5α.

*E. coli* and *S. enterica* serovar Typhimurium strains were grown in Luria-Bertani medium (LB) (10 mg tryptone $ml^{-1}$, 5 mg yeast extract $ml^{-1}$; 5 mg NaCl $ml^{-1}$) at 37°C. When required, medium was supplemented with ampicillin, tetracycline, kanamycin or chloramphenicol at final concentrations of 100, 20, 40 and 30 μg $ml^{-1}$ respectively. Electroporation was used to introduce plasmids for heterologous complementation into MSS2, XBF1 and MV501 strains (Dower *et al.*, 1988).

Motility assays. Exponentially growing cultures of *M. xanthus* were harvested (6000 *g*, room temperature (RT)) and resuspended in 1% CTT to a calculated density of $7 \times 10^9$ cells $ml^{-1}$. 5 μl aliquots of cell suspensions were spotted on 0.5% and 1.5% agar supplemented with 0.5% CTT and incubated at 32°C. Cells were visualized after 24 h using a M205FA Stereomicroscope (Leica) and imaged using a Hamamatsu ORCA-flash V2 Digital CMOS camera (Hamamatsu Photonics). Pictures were analyzed using Metamorph® v 7.5 (Molecular Devices).

Glycerol-induced sporulation assay. Assay was performed as described (Müller *et al.*, 2010) with a slightly modified protocol. Briefly, cells were cultivated in 10 ml CTT and induced at a density of $3 \times 10^8$ cells $ml^{-1}$ with glycerol to a final concentration of 0.5 M. At 0, 4 and 24 h cell morphology was observed by placing 5 μl of cells on a thin 1.5% agar TPM pad on a slide, immediately covered with a coverslip and imaged. To determine the efficiency of glycerol-induced sporulation, 5 ml of the culture were harvested (10 min, 4150 *g*, RT) after 24 h induction, resuspended in 1 ml sterile water, incubated at 50°C for 2 h, and then sonicated with 30 pulses, pulse 50%, amplitude 75% with a UP200St sonifier and microtip (Hielscher). 5 μl of the treated samples were placed on a glass slide, covered with a coverslip and imaged. Sporulation levels were determined as the number of sonication- and heat-resistant spores relative to WT using a Helber bacterial counting chamber (Hawksley, UK).

Development. Exponentially growing *M. xanthus* cultures were harvested (3 min, 6000 *g* at RT), and resuspended in MC7 buffer (10 mM MOPS pH 7.0, 1 mM CaCl2) to a calculated density of 7 × $10^9$ cells $ml^{-1}$. 10 µl aliquots of cells were placed on TPM agar (10 mM Tris-HCl pH 7.6, 1 mM $K_2HPO_4/KH_2PO_4$ pH 7.6, 8 mM $MgSO_4$), while for development in submerged culture, 50 µl aliquots were mixed with 350 µl of MC7 buffer and placed in a 24-well polystyrene plate (Falcon). Cells were visualized at the indicated time points using a M205FA Stereomicroscope (Leica) and imaged using a Hamamatsu ORCA-flash V2 Digital CMOS camera (Hamamatsu Photonics) and a DMi8 Inverted microscope and DFC9000 GT camera (Leica). After 120 h, cells were collected and incubated at 50°C for 2 h, and then sonicated as described for chemically-induced spores. Sporulation levels were determined as the number of sonication- and heat-resistant spores relative to WT using a Helber bacterial counting chamber (Hawksley, UK).

Detection of EPS accumulation. EPS accumulation was detected as in (Pérez-Burgos *et al.*, 2019). Briefly, exponentially growing cells were harvested, and resuspended in 1% CTT to a calculated density of 7 × $10^9$ cells $ml^{-1}$. 20 µl aliquots of cell suspensions were placed on 0.5% CTT 0.5% agar supplemented with 40 µg $ml^{-1}$ Congo red. The plates were incubated at 32°C and documented at 24 h.

LPS extraction and detection. LPS was extracted from *M. xanthus* and visualized by Emerald staining as previously described (Pérez-Burgos *et al.*, 2019). LPS from *S. enterica* and *E. coli* was extracted and visualized by silver staining as previously described (Marolda *et al.*, 2006, Pérez-Burgos *et al.*, 2019). For *S. enterica*, O-antigen was detected by immunoblot using rabbit *Salmonella* O antiserum group B (Difco, Beckton Dickinson ref. number 229481) (1:500) and the secondary antibody IRDye 800CW goat α-rabbit immunoglobulin G (1:10000) (LI-COR) (Pérez-Burgos *et al.*, 2019).

Cell length determination. 5 µl aliquots of exponentially growing cultures were spotted on 1.5% agar supplemented with 0.2% CTT, immediately covered with a cover slide, imaged using a DMi8 Inverted microscope and DFC9000 GT camera (Leica) and cell length determined and visualized as described (Pérez-Burgos *et al.*, 2019).

Detection of colanic acid biosynthesis. *E. coli* strains were grown at 37°C overnight on LB plates with antibiotics plus 0.2% (w/v) arabinose, when needed, to induce protein synthesis. Incubation was prolonged to 24-48 h at RT to visualize the mucoid phenotype (Furlong *et al.*, 2015).

Immunoblot analysis. Total cell extracts were prepared and FLAG-tagged proteins detected by immunoblot analysis as previously described using α-FLAG M2 monoclonal antibody (Sigma)

(1:10000) and a secondary antibody, IRDye 800CW Goat α-Mouse IgG (H+L), 0.5 mg (LI-COR) (1:10000) (Pérez-Burgos *et al.*, 2019).

Bioinformatics. The KEGG SSDB (Sequence Similarity DataBase) (Kanehisa & Goto, 2000) database was used to identify Wzx homologs (PF01943- Polysacc_synt and PF13440-Polysacc_synt_3) and WzyC (PF04932) domain containing proteins. KEGG SSDB was also used to identify homologs of Exo, Nfs and Glt proteins in other Myxococcales using a reciprocal best BlastP hit method. UniProt (The-UniProt-Consortium, 2019) and the KEGG databases were used to assign functions to proteins (Fig. 1D, Table S1). SMART (smart.embl-heidelberg.de) (Letunic *et al.*, 2015) and the Carbohydrate Active Enzymes (CAZy) database (http://www.cazy.org/) (Lombard *et al.*, 2014) were used to identify protein domains. Membrane topology was assessed by TMHMM v2.0 (Sonnhammer *et al.*, 1998) and SPOCTOPUS (Viklund *et al.*, 2008). Structure-based searches with HHPred were done using the https://toolkit.tuebingen.mpg.de/ (Zimmermann *et al.*, 2018). Clustal Omega (Chojnacki *et al.*, 2017) was used to align protein sequences.

Statistics. Statistical analyses were performed using SigmaPlot v14. All data sets were tested for a normal distribution using a Shapiro-Wilk test. For all data sets without a normal distribution, the Mann-Whitney test was applied to test for significant differences.

**Literature**

Agrebi, R., Wartel, M., Brochier-Armanet, C., and Mignot, T. (2015) An evolutionary link between capsular biogenesis and surface motility in bacteria. *Nature Reviews Microbiology* **13**: 318-326.

Alexander, D.C., and Valvano, M.A. (1994) Role of the *rfe* gene in the biosynthesis of the *Escherichia coli* O7-specific lipopolysaccharide and other O-specific polysaccharides containing N-acetylglucosamine. *Journal of Bacteriology* **176**: 7079-7084.

Amor, P.A., Yethon, J.A., Monteiro, M.A., and Whitfield, C. (1999) Assembly of the K40 antigen in *Escherichia coli*: identification of a novel enzyme responsible for addition of L-serine residues to the glycan backbone and its requirement for K40 polymerization. *Journal of Bacteriology* **181**: 772-780.

Beczała, A., Ovchinnikova, O.G., Datta, N., Mattinen, L., Knapska, K., Radziejewska-Lebrecht, J., Holst, O., and Skurnik, M. (2015) Structure and genetic basis of *Yersinia similis* serotype O:9 O-specific polysaccharide. *Innate Immunity* **21**: 3-16.

Bui, N.K., Gray, J., Schwarz, H., Schumann, P., Blanot, D., and Vollmer, W. (2009) The peptidoglycan sacculus of *Myxococcus xanthus* has unusual structural features and is degraded during glycerol-induced myxospore development. *Journal of Bacteriology* **191**: 494-505.

Burrows, L.L., and Lam, J.S. (1999) Effect of *wzx* (*rfbX*) mutations on A-band and B-band lipopolysaccharide biosynthesis in *Pseudomonas aeruginosa* O5. *Journal of Bacteriology* **181**: 973-980.

Canals, R., Jimenez, N., Vilches, S., Regue, M., Merino, S., and Tomas, J.M. (2006) The UDP N-acetylgalactosamine 4-epimerase gene is essential for mesophilic *Aeromonas hydrophila* serotype O34 virulence. *Infection and Immunity* **74**: 537-548.

Chamot-Rooke, J., Rousseau, B., Lanternier, F., Mikaty, G., Mairey, E., Malosse, C., Bouchoux, G., Pelicic, V., Camoin, L., Nassif, X., and Dumenil, G. (2007) Alternative *Neisseria* spp. type IV pilin glycosylation with a glyceramido acetamido trideoxyhexose residue. *Proceedings of the National Academy of Sciences of the United States of America* **104**: 14783-14788.

Chojnacki, S., Cowley, A., Lee, J., Foix, A., and Lopez, R. (2017) Programmatic access to bioinformatics tools from EMBL-EBI update: 2017. *Nucleic Acids Research* **45**: W550-W553.

Curtis, P.D., Atwood, J., 3rd, Orlando, R., and Shimkets, L.J. (2007) Proteins associated with the *Myxococcus xanthus* extracellular matrix. *Journal of Bacteriology* **189**: 7634-7642.

dos Santos, D.F.K., Kyaw, C.M., De Campos, T.A., Miller, R.N.G., Noronha, E.F., Bustamante, M.M.d.C., and Kruger, R., (2014) The Family Cystobacteraceae. In: The Prokaryotes: Deltaproteobacteria and Epsilonproteobacteria. E. Rosenberg, E.F. DeLong, S. Lory, E. Stackebrandt & F. Thompson (eds). Berlin, Heidelberg: Springer Berlin Heidelberg, pp. 19-40.

Dower, W.J., Miller, J.F., and Ragsdale, C.W. (1988) High efficiency transformation of *E. coli* by high voltage electroporation. *Nucleic Acids Research* **16**: 6127-6145.

Downard, J.S., and Zusman, D.R. (1985) Differential expression of protein S genes during *Myxococcus xanthus* development. *Journal of Bacteriology* **161**: 1146-1155.

Driks, A., and Eichenberger, P. (2016) The Spore Coat. *Microbiology Spectrum* **4**.

Dworkin, M. (1962) Nutritional requirements for vegetative growth of *Myxococcus xanthus*. *Journal of Bacteriology* **84**: 250-257.

Dworkin, M., and Gibson, S.M. (1964) A system for studying microbial morphogenesis: rapid formation of microcysts in *Myxococcus xanthus*. *Science* **146**: 243-244.

Dworkin, M., and Voelz, H. (1962) The formation and germination of microcysts in *Myxococcus xanthus*. *Journal of General Microbiology* **28**: 81-85.

Favrot, L., Blanchard, J.S., and Vergnolle, O. (2016) Bacterial GCN5-Related N-Acetyltransferases: From Resistance to Regulation. *Biochemistry* **55**: 989-1002.

Felsenstein, J. (1985) Confidence-Limits on Phylogenies - an Approach Using the Bootstrap. *Evolution* **39**: 783-791.

Filer, D., Kindler, S.H., and Rosenberg, E. (1977a) Myxospore coat synthesis in *Myxococcus xanthus*: enzymes associated with uridine 5'-diphosphate-N-acetylgalactosamine formation during myxospore development. *Journal of Bacteriology* **131**: 745-750.

Filer, D., White, D., Kindler, S.H., and Rosenberg, E. (1977b) Myxospore coat synthesis in *Myxococcus xanthus*: in vivo incorporation of acetate and glycine. *Journal of Bacteriology* **131**: 751-758.

Flärdh, K., and Buttner, M.J. (2009) *Streptomyces* morphogenetics: dissecting differentiation in a filamentous bacterium. *Nature Reviews Microbiology* **7**: 36-49.

Fudou, R., Jojima, Y., Iizuka, T., and Yamanaka, S. (2002) *Haliangium ochraceum* gen. nov., sp. nov. and *Haliangium tepidum* sp. nov.: novel moderately halophilic myxobacteria isolated from coastal saline environments. *Journal of General and Applied Microbiology* **48**: 109-116.

Furlong, S.E., Ford, A., Albarnez-Rodriguez, L., and Valvano, M.A. (2015) Topological analysis of the *Escherichia coli* WcaJ protein reveals a new conserved configuration for the polyisoprenyl-phosphate hexose-1-phosphate transferase family. *Scientific Reports* **5**: 9178.

Garcia, R., Gemperlein, K., and Müller, R. (2014) *Minicystis rosea* gen. nov., sp. nov., a polyunsaturated fatty acid-rich and steroid-producing soil myxobacterium. *International Journal of Systematic and Evolutionary Microbiology* **64**: 3733-3742.

Garcia, R., and Müller, R., (2014a) The Family Myxococcaceae. In: The Prokaryotes: Deltaproteobacteria and Epsilonproteobacteria. E. Rosenberg, E.F. DeLong, S. Lory, E. Stackebrandt & F. Thompson (eds). Berlin, Heidelberg: Springer Berlin Heidelberg, pp. 191-212.

Garcia, R., and Müller, R., (2014b) The Family Polyangiaceae. In: The Prokaryotes: Deltaproteobacteria and Epsilonproteobacteria. E. Rosenberg, E.F. DeLong, S. Lory, E. Stackebrandt & F. Thompson (eds). Berlin, Heidelberg: Springer Berlin Heidelberg, pp. 247-279.

Giglio, K.M., Zhu, C., Klunder, C., Kummer, S., and Garza, A.G. (2015) The enhancer binding protein Nla6 regulates developmental genes that are important for *Myxococcus xanthus* sporulation. *Journal of Bacteriology* **197**: 1276-1287.

Glover, K.J., Weerapana, E., Chen, M.M., and Imperiali, B. (2006) Direct biochemical evidence for the utilization of UDP-bacillosamine by PglC, an essential glycosyl-1-phosphate

transferase in the *Campylobacter jejuni* N-linked glycosylation pathway. *Biochemistry* **45**: 5343-5350.

Guzman, L.M., Belin, D., Carson, M.J., and Beckwith, J. (1995) Tight regulation, modulation, and high-level expression by vectors containing the arabinose PBAD promoter. *Journal of Bacteriology* **177**: 4121-4130.

Hemphill, H.E., and Zahler, S.A. (1968) Nutrition of *Myxococcus xanthus* FBa and some of its auxotrophic mutants. *Journal of Bacteriology* **95**: 1011-1017.

Hodgkin, J., and Kaiser, D. (1977) Cell-to-cell stimulation of movement in nonmotile mutants of *Myxococcus*. *Proceedings of the National Academy of Sciences of the United States of America* **74**: 2938-2942.

Holkenbrink, C., Hoiczyk, E., Kahnt, J., and Higgs, P.I. (2014) Synthesis and assembly of a novel glycan layer in *Myxococcus xanthus* spores. *Journal of Biological Chemistry* **289**: 32364-32378.

Hug, I., and Feldman, M.F. (2011) Analogies and homologies in lipopolysaccharide and glycoprotein biosynthesis in bacteria. *Glycobiology* **21**: 138-151.

Huntley, S., Hamann, N., Wegener-Feldbrugge, S., Treuner-Lange, A., Kube, M., Reinhardt, R., Klages, S., Müller, R., Ronning, C.M., Nierman, W.C., and Søgaard-Andersen, L. (2011) Comparative genomic analysis of fruiting body formation in Myxococcales. *Molecular Biology and Evolution* **28**: 1083-1097.

Inouye, M., Inouye, S., and Zusman, D.R. (1979a) Biosynthesis and self-assembly of protein S, a development specific protein of *Myxococcus xanthus*. *Proceedings of the National Academy of Sciences of the United States of America* **76**: 209-213.

Inouye, M., Inouye, S., and Zusman, D.R. (1979b) Gene expression during development of *Myxococcus xanthus*: pattern of protein synthesis. *Developmental Biology* **68**: 579-591.

Jakobczak, B., Keilberg, D., Wuichet, K., and Søgaard-Andersen, L. (2015) Contact- and protein transfer-dependent stimulation of assembly of the gliding motility machinery in *Myxococcus xanthus*. *PLoS Genetics* **11**: e1005341.

John, R.A. (1995) Pyridoxal phosphate-dependent enzymes. *Biochimics et Biophysics Acta* **1248**: 81-96.

Jorgenson, M.A., Kannan, S., Laubacher, M.E., and Young, K.D. (2016) Dead-end intermediates in the enterobacterial common antigen pathway induce morphological defects in *Escherichia coli* by competing for undecaprenyl phosphate. *Molecular Microbiology* **100**: 1-14.

Jorgenson, M.A., and Young, K.D. (2016) Interrupting biosynthesis of O antigen or the lipopolysaccharide core produces morphological defects in *Escherichia coli* by sequestering undecaprenyl phosphate. *Journal of Bacteriology* **198**: 3070-3079.

Julien, B., Kaiser, A.D., and Garza, A. (2000) Spatial control of cell differentiation in *Myxococcus xanthus*. *Proceedings of the National Academy of Sciences of the United States of America* **97**: 9098-9103.

Kaiser, D. (1979) Social gliding is correlated with the presence of pili in *Myxococcus xanthus*. *Proceedings of the National Academy of Sciences of the United States of America* **76**: 5952-5956.

Kanehisa, M., and Goto, S. (2000) KEGG: kyoto encyclopedia of genes and genomes. *Nucleic Acids Research* **28**: 27-30.

Kimura, Y., Yamashita, S., Mori, Y., Kitajima, Y., and Takegawa, K. (2011) A *Myxococcus xanthus* bacterial tyrosine kinase, BtkA, is required for the formation of mature spores. *Journal of Bacteriology* **193**: 5853-5857.

Komano, T., Furuichi, T., Teintze, M., Inouye, M., and Inouye, S. (1984) Effects of deletion of the gene for the development-specific protein S on differentiation in *Myxococcus xanthus*. *Journal of Bacteriology* **158**: 1195-1197.

Komano, T., Inouye, S., and Inouye, M. (1980) Patterns of protein production in *Myxococcus xanthus* during spore formation induced by glycerol, dimethyl sulfoxide, and phenethyl alcohol. *Journal of Bacteriology* **144**: 1076-1082.

Konovalova, A., Petters, T., and Søgaard-Andersen, L. (2010) Extracellular biology of *Myxococcus xanthus*. *FEMS Microbiology Reviews* **34**: 89-106.

Kottel, R.H., Bacon, K., Clutter, D., and White, D. (1975) Coats from *Myxococcus xanthus*: characterization and synthesis during myxospore differentiation. *Journal of Bacteriology* **124**: 550-557.

Kumar, S., Stecher, G., and Tamura, K. (2016) MEGA7: Molecular Evolutionary Genetics Analysis Version 7.0 for Bigger Datasets. *Molecular Biology and Evolution* **33**: 1870-1874.

Lee, B., Mann, P., Grover, V., Treuner-Lange, A., Kahnt, J., and Higgs, P.I. (2011) The *Myxococcus xanthus* spore cuticula Protein C is a fragment of FibA, an extracellular metalloprotease produced exclusively in aggregated cells. *PLoS ONE* **6**.

Lehrman, M.A. (1994) A family of UDP-GlcNAc/MurNAc: polyisoprenol-P GlcNAc/MurNAc-1-P transferases. *Glycobiology* **4**: 768-771.

Leng, X., Zhu, W., Jin, J., and Mao, X. (2011) Evidence that a chaperone-usher-like pathway of *Myxococcus xanthus* functions in spore coat formation. *Microbiology* **157**: 1886-1896.

Letunic, I., Doerks, T., and Bork, P. (2015) SMART: recent updates, new developments and status in 2015. *Nucleic Acids Research* **43**: D257-260.

Licking, E., Gorski, L., and Kaiser, D. (2000) A common step for changing cell shape in fruiting body and starvation-independent sporulation in *Myxococcus xanthus. Journal of Bacteriology* **182**: 3553-3558.

Lombard, V., Golaconda Ramulu, H., Drula, E., Coutinho, P.M., and Henrissat, B. (2014) The Carbohydrate-active enzymes database (CAZy) in 2013. *Nucleic Acids Research* **42**: D490–D495.

Lu, A., Cho, K., Black, W.P., Duan, X.Y., Lux, R., Yang, Z., Kaplan, H.B., Zusman, D.R., and Shi, W. (2005) Exopolysaccharide biosynthesis genes required for social motility in *Myxococcus xanthus*. *Molecular Microbiology* **55**: 206-220.

Luciano, J., Agrebi, R., Le Gall, A.V., Wartel, M., Fiegna, F., Ducret, A., Brochier-Armanet, C., and Mignot, T. (2011) Emergence and modular evolution of a novel motility machinery in bacteria. *PLoS Genetics* **7**: e1002268.

Marolda, C.L., Lahiry, P., Vines, E., Saldias, S., and Valvano, M.A. (2006) Micromethods for the characterization of lipid A-core and O-antigen lipopolysaccharide. *Methods in Molecular Biology* **347**: 237-252.

Marolda, C.L., Vicarioli, J., and Valvano, M.A. (2004) Wzx proteins involved in biosynthesis of O antigen function in association with the first sugar of the O-specific lipopolysaccharide subunit. *Microbiology* **150**: 4095-4105.

McCleary, W.R., Esmon, B., and Zusman, D.R. (1991) *Myxococcus xanthus* protein C is a major spore surface protein. *Journal of Bacteriology* **173**: 2141-2145.

McKenney, P.T., Driks, A., and Eichenberger, P. (2013) The *Bacillus subtilis* endospore: assembly and functions of the multilayered coat. *Nature Reviews Microbiology* **11**: 33-44.

Merino, S., Jimenez, N., Molero, R., Bouamama, L., Regue, M., and Tomas, J.M. (2011) A UDP-HexNAc:polyprenol-P GalNAc-1-P transferase (WecP) representing a new subgroup of the enzyme family. *Journal of Bacteriology* **193**: 1943-1952.

Mohr, K.I., Garcia, R.O., Gerth, K., Irschik, H., and Müller, R. (2012) *Sandaracinus amylolyticus* gen. nov., sp. nov., a starch-degrading soil myxobacterium, and description of *Sandaracinaceae* fam. nov. *International Journal of Systematic and Evolutionary Microbiology* **62**: 1191-1198.

Morona, R., Purins, L., Tocilj, A., Matte, A., and Cygler, M. (2009) Sequence-structure relationships in polysaccharide co-polymerase (PCP) proteins. *Trends Biochem Sci* **34**: 78-84.

Müller, F.D., Schink, C.W., Hoiczyk, E., Cserti, E., and Higgs, P.I. (2012) Spore formation in *Myxococcus xanthus* is tied to cytoskeleton functions and polysaccharide spore coat deposition. *Molecular Microbiology* **83**: 486-505.

Müller, F.D., Treuner-Lange, A., Heider, J., Huntley, S.M., and Higgs, P.I. (2010) Global transcriptome analysis of spore formation in *Myxococcus xanthus* reveals a locus necessary for cell differentiation. *BMC Genomics* **11**: 264.

Nan, B., Bandaria, J.N., Moghtaderi, A., Sun, I.-H., Yildiz, A., and Zusman, D.R. (2013) Flagella stator homologs function as motors for myxobacterial gliding motility by moving in helical

trajectories. *Proceedings of the National Academy of Sciences of the United States of America* **110**: E1508-E1513.

Noland, B.W., Newman, J.M., Hendle, J., Badger, J., Christopher, J.A., Tresser, J., Buchanan, M.D., Wright, T.A., Rutter, M.E., Sanderson, W.E., Muller-Dieckmann, H.J., Gajiwala, K.S., and Buchanan, S.G. (2002) Structural studies of *Salmonella typhimurium* ArnB (PmrH) aminotransferase: a 4-amino-4-deoxy-L-arabinose lipopolysaccharide-modifying enzyme. *Structure* **10**: 1569-1580.

O'Connor, K.A., and Zusman, D.R. (1997) Starvation-independent sporulation in *Myxococcus xanthus* involves the pathway for beta-lactamase induction and provides a mechanism for competitive cell survival. *Molecular Microbiology* **24**: 839-850.

Otani, M., Kozuka, S., Xu, C., Umezawa, C., Sano, K., and Inouye, S. (1998) Protein W, a spore-specific protein in *Myxococcus xanthus*, formation of a large electron-dense particle in a spore. *Molecular Microbiology* **30**: 57-66.

Patel, K.B., Furlong, S.E., and Valvano, M.A. (2010) Functional analysis of the C-terminal domain of the WbaP protein that mediates initiation of O antigen synthesis in *Salmonella enterica*. *Glycobiology* **20**: 1389-1401.

Patel, K.B., Toh, E., Fernandez, X.B., Hanuszkiewicz, A., Hardy, G.G., Brun, Y.V., Bernards, M.A., and Valvano, M.A. (2012) Functional characterization of UDP-glucose:undecaprenyl-phosphate glucose-1-phosphate transferases of *Escherichia coli* and *Caulobacter crescentus*. *Journal of Bacteriology* **194**: 2646-2657.

Pérez-Burgos, M., García-Romero, I., Jung, J., Valvano, M.A., and Søgaard-Andersen, L. (2019) Identification of the lipopolysaccharide O-antigen biosynthesis priming enzyme and the O-antigen ligase in *Myxococcus xanthus*: Critical role of LPS O-antigen in motility and development. *Molecular Microbiology* **112**: 1178-1198.

Power, P.M., Roddam, L.F., Dieckelmann, M., Srikhanta, Y.N., Tan, Y.C., Berrington, A.W., and Jennings, M.P. (2000) Genetic characterization of pilin glycosylation in Neisseria meningitidis. *Microbiology* **146 ( Pt 4)**: 967-979.

Raetz, C.R., and Whitfield, C. (2002) Lipopolysaccharide endotoxins. *Annual Review of Biochemistry* **71**: 635-700.

Ranjit, D.K., and Young, K.D. (2016) Colanic acid intermediates prevent *de novo* shape recovery of *Escherichia coli* spheroplasts, calling into question biological roles previously attributed to colanic acid. *Journal of Bacteriology* **198**: 1230-1240.

Rehm, B.H. (2010) Bacterial polymers: biosynthesis, modifications and applications. *Nature Reviews Microbiology* **8**: 578-592.

Reichenbach, H. (1999) The ecology of the myxobacteria. *Environmental Microbiology* **1**: 15-21.

Reith, J., and Mayer, C. (2011) Characterization of a glucosamine/glucosaminide N-acetyltransferase of *Clostridium acetobutylicum*. *Journal of Bacteriology* **193**: 5393-5399.

Sadler, W., and Dworkin, M. (1966) Induction of cellular morphogenesis in *Myxococcus xanthus*. II. Macromolecular synthesis and mechanism of inducer action. *Journal of Bacteriology* **91**: 1520-1525.

Saitou, N., and Nei, M. (1987) The Neighbor-Joining Method - a New Method for Reconstructing Phylogenetic Trees. *Molecular Biology and Evolution* **4**: 406-425.

Saldías, M.S., Patel, K., Marolda, C.L., Bittner, M., Contreras, I., and Valvano, M.A. (2008) Distinct functional domains of the *Salmonella enterica* WbaP transferase that is involved in the initiation reaction for synthesis of the O antigen subunit. *Microbiology* **154**: 440-453.

Sanford, R.A., Cole, J.R., and Tiedje, J.M. (2002) Characterization and description of *Anaeromyxobacter dehalogenans* gen. nov., sp. nov., an aryl-halorespiring facultative anaerobic myxobacterium. *Applied and Environment Microbiology* **68**: 893-900.

Schäffer, C., Wugeditsch, T., Messner, P., and Whitfield, C. (2002) Functional expression of enterobacterial O-polysaccharide biosynthesis enzymes in *Bacillus subtilis*. *Applied and Environment Microbiology* **68**: 4722-4730.

Schild, S., Lamprecht, A.K., and Reidl, J. (2005) Molecular and functional characterization of O antigen transfer in *Vibrio cholerae*. *Journal of Biological Chemistry* **280**: 25936-25947.

Schmid, J., Sieber, V., and Rehm, B. (2015) Bacterial exopolysaccharides: Biosynthesis pathways and engineering strategies. *Frontiers in Microbiology* **6**.

Schumacher, D., Bergeler, S., Harms, A., Vonck, J., Huneke-Vogt, S., Frey, E., and Sogaard-Andersen, L. (2017) The PomXYZ proteins self-organize on the bacterial nucleoid to stimulate cell division. *Developmental Cell* **41**: 299-314 e213.

Schumacher, D., and Søgaard-Andersen, L. (2017) Regulation of cell polarity in motility and cell division in *Myxococcus xanthus*. *Annual Review of Microbiology* **71**: 61-78.

Shi, X., Wegener-Feldbrugge, S., Huntley, S., Hamann, N., Hedderich, R., and Søgaard-Andersen, L. (2008) Bioinformatics and experimental analysis of proteins of two-component systems in *Myxococcus xanthus*. *Journal of Bacteriology* **190**: 613-624.

Sigle, S., Ladwig, N., Wohlleben, W., and Muth, G. (2015) Synthesis of the spore envelope in the developmental life cycle of *Streptomyces coelicolor*. *International Journal of Medical Microbiology* **305**: 183-189.

Sonnhammer, E.L., von Heijne, G., and Krogh, A. (1998) A hidden Markov model for predicting transmembrane helices in protein sequences. *Proceedings of International Conference on Intelligent Systems for Molecular Biology* **6**: 175-182.

Sprecher, K.S., Hug, I., Nesper, J., Potthoff, E., Mahi, M.A., Sangermani, M., Kaever, V., Schwede, T., Vorholt, J., and Jenal, U. (2017) Cohesive properties of the *Caulobacter crescentus* holdfast adhesin are regulated by a novel c-di-GMP effector protein. *mBio* **8**.

Sun, M., Wartel, M., Cascales, E., Shaevitz, J.W., and Mignot, T. (2011) Motor-driven intracellular transport powers bacterial gliding motility. *Proceedings of the National Academy of Sciences of the United States of America* **108**: 7559-7564.

Sutherland, I.W., and Mackenzie, C.L. (1977) Glucan common to the microcyst walls of cyst-forming bacteria. *Journal of Bacteriology* **129**: 599-605.

Tan, I.S., and Ramamurthi, K.S. (2014) Spore formation in *Bacillus subtilis*. *Environmental Microbiology Reports* **6**: 212-225.

The-UniProt-Consortium (2019) UniProt: a worldwide hub of protein knowledge. *Nucleic Acids Research* **47**: D506-515.

Treuner-Lange, A., Aguiluz, K., van der Does, C., Gomez-Santos, N., Harms, A., Schumacher, D., Lenz, P., Hoppert, M., Kahnt, J., Munoz-Dorado, J., and Sogaard-Andersen, L. (2013)

PomZ, a ParA-like protein, regulates Z-ring formation and cell division in *Myxococcus xanthus*. *Molecular Microbiology* **87**: 235-253.

Treuner-Lange, A., Macia, E., Guzzo, M., Hot, E., Faure, L.M., Jakobczak, B., Espinosa, L., Alcor, D., Ducret, A., Keilberg, D., Castaing, J.P., Lacas Gervais, S., Franco, M., Søgaard-Andersen, L., and Mignot, T. (2015) The small G-protein MglA connects to the MreB actin cytoskeleton at bacterial focal adhesions. *Journal of Cell Biology* **210**: 243-256.

Ud-Din, A.I., Liu, Y.C., and Roujeinikova, A. (2015) Crystal structure of *Helicobacter pylori* pseudaminic acid biosynthesis N-acetyltransferase PseH: implications for substrate specificity and catalysis. *PLoS ONE* **10**: e0115634.

Ueki, T., and Inouye, S. (2005) Identification of a gene involved in polysaccharide export as a transcription target of FruA, an essential factor for *Myxococcus xanthus* development. *Journal of Biological Chemistry* **280**: 32279-32284.

Valvano, M.A. (2008) Undecaprenyl phosphate recycling comes out of age. *Molecular Microbiology* **67**: 232-235.

Valvano, M.A. (2011) Common themes in glycoconjugate assembly using the biogenesis of O-antigen lipopolysaccharide as a model system. *Biochemistry (Mosc)* **76**: 729-735.

Valvano, M.A., and Crosa, J.H. (1984) Aerobactin iron transport genes commonly encoded by certain ColV plasmids occur in the chromosome of a human invasive strain of *Escherichia coli* K1. *Infection and Immunity* **46**: 159-167.

Valvano, M.A., Furlong, S.E., and Patel, K.B., (2011) Genetics, biosynthesis and assembly of O-antigen. In: Bacterial Lipopolysaccharides: Structure, Chemical Synthesis, Biogenesis and Interaction with Host Cells. Y.A. Knirel & M.A. Valvano (eds). Vienna: Springer Vienna, pp. 275-310.

Viklund, H., Bernsel, A., Skwark, M., and Elofsson, A. (2008) SPOCTOPUS: a combined predictor of signal peptides and membrane protein topology. *Bioinformatics* **24**: 2928-2929.

Wan, Z., Brown, P.J., Elliott, E.N., and Brun, Y.V. (2013) The adhesive and cohesive properties of a bacterial polysaccharide adhesin are modulated by a deacetylase. *Molecular Microbiology* **88**: 486-500.

Wartel, M., Ducret, A., Thutupalli, S., Czerwinski, F., Le Gall, A.V., Mauriello, E.M., Bergam, P., Brun, Y.V., Shaevitz, J., and Mignot, T. (2013) A versatile class of cell surface directional motors gives rise to gliding motility and sporulation in *Myxococcus xanthus*. *PLoS Biology* **11**: e1001728.

Watson, B.F., and Dworkin, M. (1968) Comparative intermediary metabolism of vegetative cells and microcysts of *Myxococcus xanthus*. *Journal of Bacteriology* **96**: 1465-1473.

Wu, S.S., and Kaiser, D. (1996) Markerless deletions of *pil* genes in *Myxococcus xanthus* generated by counterselection with the *Bacillus subtilis sacB* gene. *Journal of Bacteriology* **178**: 5817-5821.

Wu, S.S., and Kaiser, D. (1997) Regulation of expression of the *pilA* gene in *Myxococcus xanthus*. *Journal of Bacteriology* **179**: 7748-7758.

Yamamoto, E., Muramatsu, H., and Nagai, K. (2014) *Vulgatibacter incomptus* gen. nov., sp. nov. and *Labilithrix luteola* gen. nov., sp. nov., two myxobacteria isolated from soil in Yakushima Island, and the description of *Vulgatibacteraceae* fam. nov., *Labilitrichaceae* fam. nov. and *Anaeromyxobacteraceae* fam. nov. *International Journal of Systematic and Evolutionary Microbiology* **64**: 3360-3368.

Yang, Z., Geng, Y., Xu, D., Kaplan, H.B., and Shi, W. (1998) A new set of chemotaxis homologues is essential for *Myxococcus xanthus* social motility. *Molecular Microbiology* **30**: 1123-1130.

Zhang, Y., Ducret, A., Shaevitz, J., and Mignot, T. (2012) From individual cell motility to collective behaviors: insights from a prokaryote, *Myxococcus xanthus*. *FEMS Microbiology Reviews* **36**: 149-164.

Zimmermann, L., Stephens, A., Nam, S.-Z., Rau, D., Kübler, J., Lozajic, M., Gabler, F., Söding, J., Lupas, A.N., and Alva, V. (2018) A completely reimplemented MPI bioinformatics toolkit with a new HHpred server at its core. *Journal of Molecular Biology* **430**: 2237-2243.

**Figure 1.** Model and expression analysis of gene clusters involved in spore coat polysaccharide synthesis.
(A) Current model for spore coat polysaccharide synthesis in *M. xanthus* (see text). Proteins indicated in stippled lines have not been identified. Note that the number of GTs is unknown. Right panel, the colour code indicates predicted functions and is used throughout all figures. (B, E) Transcription pattern of indicated genes in response to chemical-induction of sporulation with 0.5 M glycerol (+gly) based on data from (Müller *et al.*, 2010) and shown as log2-fold change compared to cells in the absence of glycerol (-gly). Note that the expression pattern of the genes in the *exo* I gene cluster were previously published (Müller *et al.*, 2010, Müller *et al.*, 2012) and are included for comparison. (C) Domain and TMH prediction of ExoM (MXAN_3260) and ExoJ (MXAN_3026) where domains are indicated in red and green, respectively. Grey rectangles indicate TMHs, red and black lines indicate periplasmic and cytoplasmic regions, respectively. Numbers indicate domain borders. (D) *exo* gene cluster I, II and III. Genes are drawn to scale and MXAN number and gene name are indicated (see also Table S1). Gene orientation is indicated by the direction of arrows. Note that the *exoJ-K*, *exoL-M* and *exoN-P* genes are likely in operons. The *exoA-I* genes form an operon (Müller *et al.*, 2012). Gene coordinates are relative to the first nucleotide of the first gene in an operon and are indicated by the same gene colour, except for *exoE*, for which coordinates are indicated relative to its first nucleotide. DNA fragments comprising promoter and structural gene used in complementation experiments are indicated by a line above the corresponding region/s.

**Figure 2.** Chemically induced sporulation in Δ*exo* mutants.
(A) Sporulation was induced by addition of glycerol to a final concentration of 0.5 M. At 0, 4 and 24 h, cell morphology was observed by phase contrast microscopy. In images labelled resistant spores, cells were exposed to sonic and heat treatment before microscopy. Sporulation frequency after sonic and heat treatment is indicated as the mean ± standard deviation from three biological experiments relative to WT. $P_{nat}$ is short for the native promoter and is used throughout the study. Scale bars, 5 μm. (B) Quantification of cell morphology at 24 h before sonic and heat treatment relative to WT (100%); n = 300 combined from three biological replicates.

**Figure 3.** EPS and LPS synthesis, and cell length determination in the Δ*exo* mutants.
(A) Determination of EPS accumulation. 20 μl of cell suspensions at 7 × $10^9$ cells $ml^{-1}$ were spotted on 0.5% agar supplemented with 0.5% CTT and Congo red and incubated at 32°C for 24

h. The Ω*difE* mutant served as a negative control. (B) Detection of LPS O-antigen. Extracted LPS samples from the same number of cells were separated by SDS-PAGE and visualized using Pro-Q Emerald 300. The Δ*wbaP* mutant served as a negative control. (C) Cell length determination. Cell length distribution is shown in a violin plot. Each violin indicates the probability density of the data at different cell lengths. Mean and median values are represented by a continuous and dashed line, respectively. For each strain, mean cell length ± standard deviation is indicated; n =800 combined from four biological replicates. Samples were compared using a Mann-Whitney test, * indicates *p* value < 0.05 and ns, not significant.

**Figure 4.** ExoE has GalNAc-1-P transferase activity.
(A) Domain and TMH prediction for $WbaP_{Se}$, $WcaJ_{Ec}$, $WecA_{Ec}$ and ExoE. Grey rectangles indicate TMH. Numbers indicate domain borders. (B) Topology predictions for ExoE. The catalytic PF02397 domain is indicated in blue and conserved amino acids important for structure or activity are marked with orange and red, respectively. The amino acid sequence alignment of ExoE with $WbaP_{Se}$ is shown in Fig. S3. (C-G) Heterologous complementation experiments to characterize ExoE specificity. (C) *E.coli* XBF1 (Δ$wcaJ_{Ec}$) containing pWQ499 (*rcsA*$^+$) was transformed with the indicated plasmids and plated on LB agar in the absence or presence of 0.2% arabinose (ara) to induce gene expression. Cells were incubated for 24 h at 37°C and then 24 h at room temperature before scoring the mucoid phenotype. (D, E) Silver-stained polyacrylamide gels of LPS extracted from the *E. coli wecA*::Tn*10* mutant strain MV501 carrying the indicated plasmids. In (E), MV501 also contained the plasmid pGEMT-Gne, which encodes the UDP-GlcNAc/UDP-GalNAc epimerase $Gne_{Ah}$. VW187 is the parental *wecA*$^+$ strain. Arabinose was added as indicated. (F) Silver-stained polyacrylamide gel and (G) immunoblot with rabbit *Salmonella* group B O-antigen antiserum of LPS extracted from *S. enterica* LT2 (WT) and the MSS2 Δ$wbaP_{Se}$ mutant carrying the indicated plasmids. Arabinose was added as indicated.

**Figure 5.** Analysis of *exo*, *nfs* and *glt* gene occurrence and organization in myxobacteria.
(A) Taxonomic distribution, co-occurrence and synteny of the *exo*, *nfs* and *glt* genes in Myxococcales. Left, 16S rRNA tree of Myxococcales with fully sequenced genomes. Family and suborder classification are indicated. Genome size is indicated on the right. Used strains are listed in Table S2. S, species that form spores; (S), tested for sporulation but with ambiguous results; NT, sporulation not tested; N, sporulation tested and not observed (Yamamoto *et al.*, 2014, Garcia *et al.*, 2014, Mohr *et al.*, 2012, Fudou *et al.*, 2002, Garcia & Müller, 2014a, Garcia & Müller, 2014b, Sanford *et al.*, 2002, dos Santos *et al.*, 2014). For the *exo*, *nfs* and *glt* gene

clusters, a reciprocal best BlastP hit method was used to identify orthologs. Generally, the *exo* gene clusters are marked in green (cluster II), blue (cluster I) and red (cluster III) and the *nfs* and *glt* gene clusters in orange (*nfs*), light brown (*glt* cluster I) and dark brown (*glt* cluster II). To evaluate gene proximity and cluster conservation, 10 genes were considered as the maximum distance for a gene to be in a cluster. Genes found in the same cluster are marked with the same colour. If two or three gene clusters are within a distance of <10 genes, all genes are marked in the same colour (e.g. two of the *exo* clusters in *V. incomptus*, all three *exo* clusters in Anaeromyxobacteraceae and the *glt* clusters in Anaeromyxobacteraceae, Nannocystineae and Sorangineae). Light grey indicates a conserved gene that is found somewhere else on the genome (>10 genes away from a cluster); dark grey and black indicate conservation of the marked genes but in a separate cluster; a cross indicates no homolog found. Note that the *nfsB* gene in *L. luteola* DSM 27648 is found in close proximity to the *gltC*, *glG* and *gltI* genes and is most likely a *gltB* homolog. (B) Nfs and Glt gene clusters in *M. xanthus*. Genes are not drawn to scale, MXAN number or gene name are indicated and gene orientation is indicated by arrows. The tree in A was prepared in MEGA7 (Kumar *et al.*, 2016) using the Neighbor-Joining method (Saitou & Nei, 1987). Bootstrap values (500 replicates) are shown next to the branches (Felsenstein, 1985).

**Figure 6.** Model of spore coat polysaccharide biosynthesis in *M. xanthus*. Colour code indicates predicted functions. Stippled lines indicate that the site of action is hypothetical and remains to be determined experimentally. See Discussion for details. ExoE adds the first sugar of the repeat unit (blue), which is likely GalNAc, followed by addition of monosaccharides (Glc and GalNAc) by the GTs (yellow).

**Table 1.** Motility and starvation-induced sporulation phenotypes of the *exo* mutants.

| Strain genotype | T4P-dependent motility | Gliding motility | Sporulation on TPM agar[1] | Sporulation in submerged culture[1] |
|---|---|---|---|---|
| WT | + | + | 100±50% | 100±40% |
| Δ*exoE* | + | + | <3% (143±59%) | <3% (89±17%) |
| Δ*exoM* | + | + | <3% (185±39%) | <3% 115±33% |
| Δ*exoJ* | + | + | <3% (118±33%) | <3% (91±33%) |
| Δ*exoK* | + | + | <3% (108±38%) | <3% (82±26%) |
| Δ*exoL* | + | + | <3% (97±27%) | <3% (64±13%) |
| Δ*exoN* | + | + | 54±12% (69±30%) | 39±26% (45±10%) |
| Δ*exoO* | + | + | <3% (68±18%) | <3% (71±29%) |
| Δ*exoP* | + | + | <3% (106±70%) | <3% (114±42%) |

[1] Sporulation efficiency after heat and sonic treatment is indicated as the mean ± standard deviation from three biological replicates relative to WT. Numbers in brackets indicate sporulation levels in the complementation strains.

**Table 2.** Strains used in this work

| Strain | Genotype | Reference |
|---|---|---|
| ***M. xanthus*** | | |
| DK1622 | Wildtype | (Kaiser, 1979) |
| DK10410 | Δ*pilA* | (Wu & Kaiser, 1997) |
| SA5923 | Δ*aglQ* | (Jakobczak *et al.*, 2015) |
| SW501 | *difE*::Km$^r$ | (Yang *et al.*, 1998) |
| SA7450 | Δ*wbaP* | (Pérez-Burgos *et al.*, 2019) |
| SA7495 | Δ*exoE* | (Pérez-Burgos *et al.*, 2019) |
| SA8534 | Δ*exoE attB*::pMP136 ($P_{nat}$ *exoE*) | This study |
| SA7455 | Δ*MXAN_3026* | This study |
| SA7489 | Δ*MXAN_3026 attB*::pJJ18 ($P_{nat}$ *MXAN_3026*) | This study |
| SA8507 | Δ*MXAN_3260* | This study |
| SA8502 | Δ*MXAN_3260 attB*::pJJ18 ($P_{nat}$ *MXAN_3260*) | This study |
| SA8516 | Δ*MXAN_3027* | This study |
| SA8523 | Δ*MXAN_3027 attB*::pMP125 ($P_{nat}$ *MXAN_3027*) | This study |
| SA8519 | Δ*MXAN_3259* | This study |
| SA8522 | Δ*MXAN_3259 attB*::pMP126 ($P_{nat}$ *MXAN_3259*) | This study |
| SA8527 | Δ*MXAN_3261* | This study |
| SA8528 | Δ*MXAN_3261 attB*::pMP133 ($P_{nat}$ *MXAN_3261*) | This study |
| SA8547 | Δ*MXAN_3262* | This study |
| SA8548 | Δ*MXAN_3262 attB*::pMP134 ($P_{nat}$ *MXAN_3262*) | This study |
| SA8517 | Δ*MXAN_3263* | This study |
| SA8531 | Δ*MXAN_3263 attB*::pMP135 ($P_{nat}$ *MXAN_3263*) | This study |
| ***E. coli*** | | |
| DH5α | F$^-$ φ80*lacZ*ΔM15 *endA recA hsdR*($r_K^-$ $m_K^-$) *nupG thi glnV deoR gyrA relA1* Δ(*lacZYA-argF*)U169 | Lab stock |
| Mach1 | Δ*recA*1398 *endA*1 *tonA* Φ80Δ*lacM*15 Δ*lacX*74 *hsdR*($r_K^-$ $m_K^+$) | Invitrogen |
| XBF1 | W3110*,* Δ*wcaJ::aph*, Km$^r$ | (Patel *et al.*, 2012) |
| VW187 | O7:K1, clinical isolate | (Valvano & Crosa, 1984) |
| MV501 | VW187, *wecA*::Tn10 Tc$^r$ | (Alexander & Valvano, |

| | | |
|---|---|---|
| | | 1994) |
| ***Salmonella*** | | |
| LT2 | WT, *S. enterica* serovar Typhimurium | S. Maloy |
| MSS2 | LT2, Δ*wbaP*::*cat* $Cm^r$ | (Saldías *et al.*, 2008) |

**Table 3. Plasmids used in this work.**

| Plasmid | Description | Reference |
|---|---|---|
| pBJ114 | Km$^r$ *galK* | (Julien *et al.*, 2000) |
| pSWU30 | Tet$^r$ | (Wu & Kaiser, 1997) |
| pBAD24 | Cloning vector with arabinose inducible promoter, Amp$^r$ | (Guzman *et al.*, 1995) |
| pBADNTF | pBAD24 for N-terminal FLAG fusion, Amp$^r$ | (Marolda *et al.*, 2004) |
| pLA3 | pBADNTF, *wcaJ*, Amp$^r$ | (Furlong *et al.*, 2015) |
| pSM13 | pUC18, *wbaP* from *S. enterica* Ty2 containing a 1 bp deletion at position 583 and a 2 bp deletion at position 645. This causes a frame shift at WbaP I194 and frame restoration at Y215, Amp$^r$ | (Saldías *et al.*, 2008) |
| pJD132 | pBluescript SK, *wbaP* and flanking sequences from *E. coli* O9:K30, Amp$^r$ | (Schäffer *et al.*, 2002) |
| pWQ499 | pKV102 containing *rcsAK30*, Tet$^r$ | C. Whitfield |
| pMAV11 | pACYC184, containing *rfe*, Cm$^r$ | (Alexander & Valvano, 1994) |
| pSEF88 | pBAD24 expressing $_{FLAG}$WecP from *Aeromonas hydrophila* AH-3, Amp$^r$ | S. Furlong |
| pGEMT-Gne | pGEMT encoding *gne* from *Aeromonas hydrophila* AH-3, Amp$^r$ | (Canals *et al.*, 2006) |
| pJJ5 | pBJ114, in-frame deletion construct for *MXAN_3026* Km$^r$ | This work |
| pJJ18 | pSWU30, $P_{nat}$ *MXAN_3026* Tet$^r$ | This work |
| pMP113 | pBJ114, in-frame deletion construct for *MXAN_3260* Km$^r$ | This work |
| pMP118 | pSWU30, $P_{nat}$ *MXAN_3260* Tet$^r$ | This work |
| pMP120 | pBJ114, in-frame deletion construct for *MXAN_3027* Km$^r$ | This work |
| pMP121 | pBJ114, in-frame deletion construct for *MXAN_3259* Km$^r$ | This work |
| pMP123 | pBJ114, in-frame deletion construct for | This work |

| | | |
|---|---|---|
| | *MXAN_3263* Km$^r$ | |
| pMP125 | pSWU30, P$_{nat}$ *MXAN_3027* Tet$^r$ | This work |
| pMP126 | pSWU30, P$_{nat}$ *MXAN_3259* Tet$^r$ | This work |
| pMP131 | pBJ114, in-frame deletion construct for *MXAN_3261* Km$^r$ | This work |
| pMP133 | pSWU30, P$_{nat}$ *MXAN_3261* Tet$^r$ | This work |
| pMP134 | pSWU30, P$_{nat}$ *MXAN_3262* Tet$^r$ | This work |
| pMP135 | pSWU30, P$_{nat}$ *MXAN_3263* Tet$^r$ | This work |
| pMP136 | pSWU30, P$_{nat}$ *exoE* Tet$^r$ | This work |
| pMP144 | pBJ114, in-frame deletion construct for Nterminal *MXAN_3262* Km$^r$ | This work |
| pMP147 | pBADNTF, *exoE* Amp$^r$ | This work |
| pMP158 | pBAD24, *exoE* Amp$^r$ | This work |

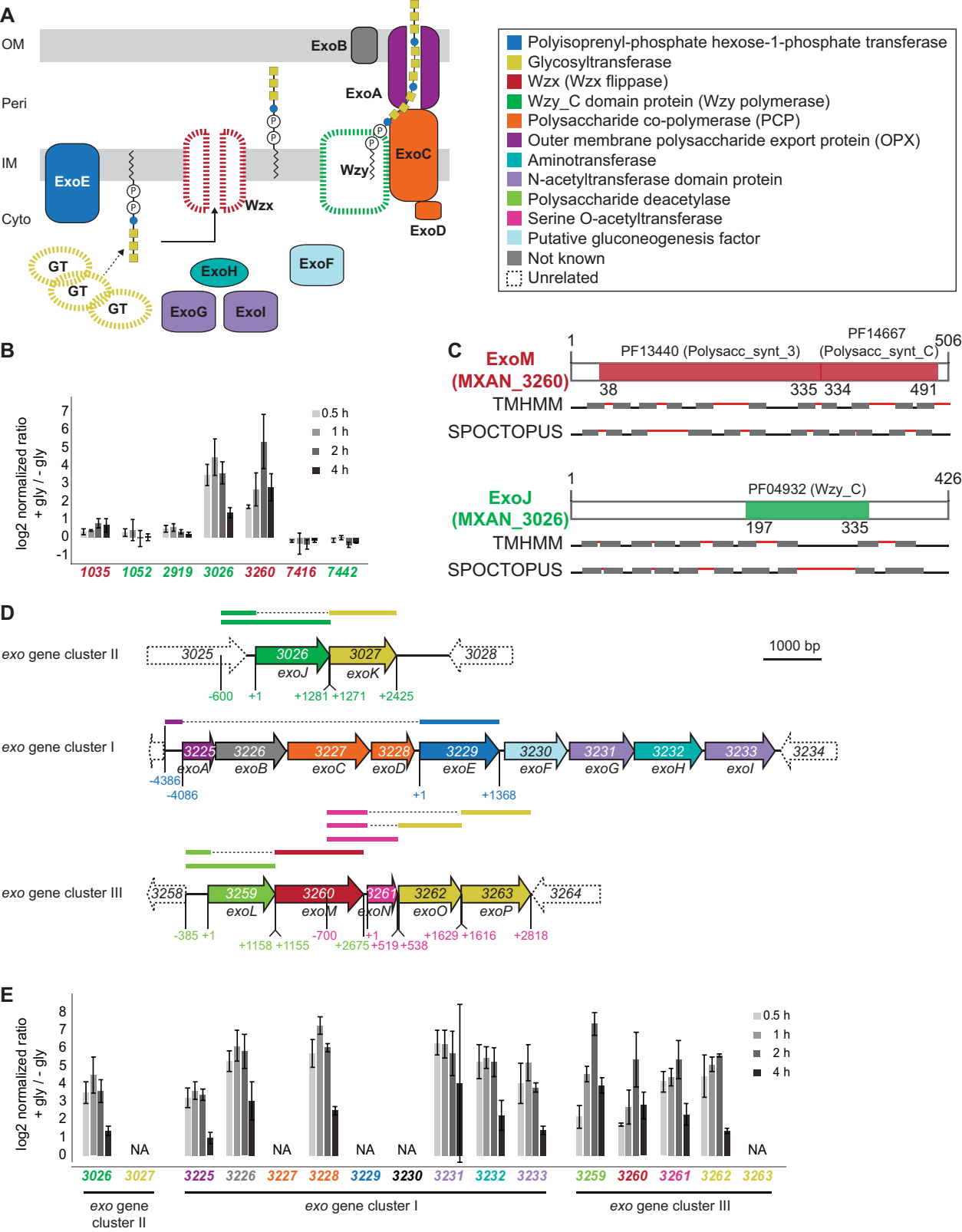
A
OM
Peri
IM
Cyto
ExoB
ExoA
ExoC
ExoD
ExoE
Wzx
Wzy
GT
GT
GT
ExoH
ExoG
ExoI
ExoF
Polyisoprenyl-phosphate hexose-1-phosphate transferase
Glycosyltransferase
Wzx (Wzx flippase)
Wzy_C domain protein (Wzy polymerase)
Polysaccharide co-polymerase (PCP)
Outer membrane polysaccharide export protein (OPX)
Aminotransferase
N-acetyltransferase domain protein
Polysaccharide deacetylase
Serine O-acetyltransferase
Putative gluconeogenesis factor
Not known
Unrelated
B
log2 normalized ratio + gly / - gly
0.5 h
1 h
2 h
4 h
1035 1052 2919 3026 3260 7416 7442
C
ExoM (MXAN_3260)
PF13440 (Polysacc_synt_3)
PF14667 (Polysacc_synt_C)
TMHMM
SPOCTOPUS
ExoJ (MXAN_3026)
PF04932 (Wzy_C)
D
exo gene cluster II
exo gene cluster I
exo gene cluster III
1000 bp
E
log2 normalized ratio + gly / - gly
NA
exo gene cluster II
exo gene cluster I
exo gene cluster III

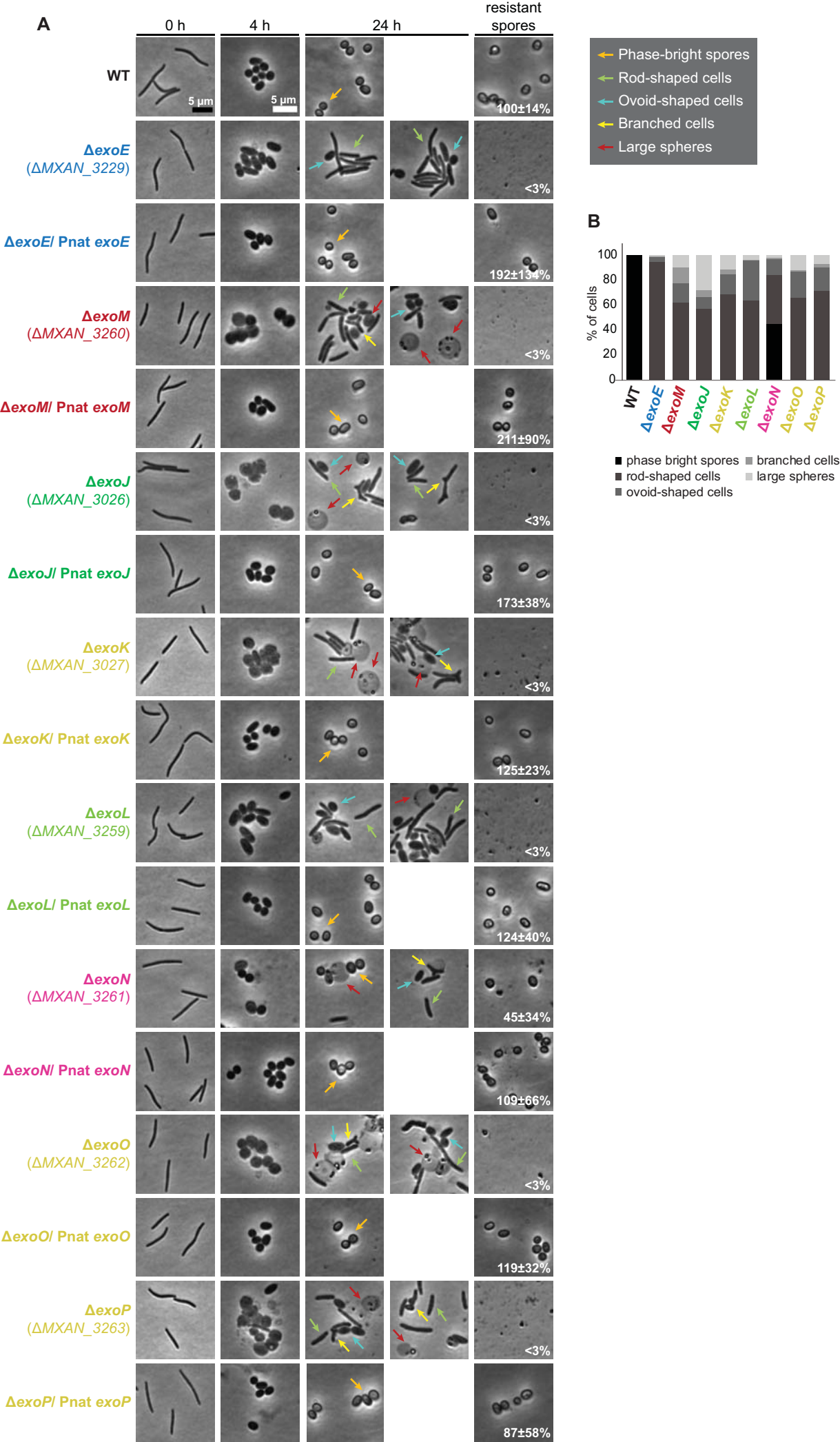
A
0 h
4 h
24 h
resistant spores
WT
5 µm
5 µm
100±14%
ΔexoE (ΔMXAN_3229)
<3%
ΔexoE/ Pnat exoE
192±134%
ΔexoM (ΔMXAN_3260)
<3%
ΔexoM/ Pnat exoM
211±90%
ΔexoJ (ΔMXAN_3026)
<3%
ΔexoJ/ Pnat exoJ
173±38%
ΔexoK (ΔMXAN_3027)
<3%
ΔexoK/ Pnat exoK
125±23%
ΔexoL (ΔMXAN_3259)
<3%
ΔexoL/ Pnat exoL
124±40%
ΔexoN (ΔMXAN_3261)
45±34%
ΔexoN/ Pnat exoN
109±66%
ΔexoO (ΔMXAN_3262)
<3%
ΔexoO/ Pnat exoO
119±32%
ΔexoP (ΔMXAN_3263)
<3%
ΔexoP/ Pnat exoP
87±58%
Phase-bright spores
Rod-shaped cells
Ovoid-shaped cells
Branched cells
Large spheres
B
% of cells
100
80
60
40
20
0
WT
ΔexoE
ΔexoM
ΔexoJ
ΔexoK
ΔexoL
ΔexoN
ΔexoO
ΔexoP
phase bright spores
rod-shaped cells
ovoid-shaped cells
branched cells
large spheres

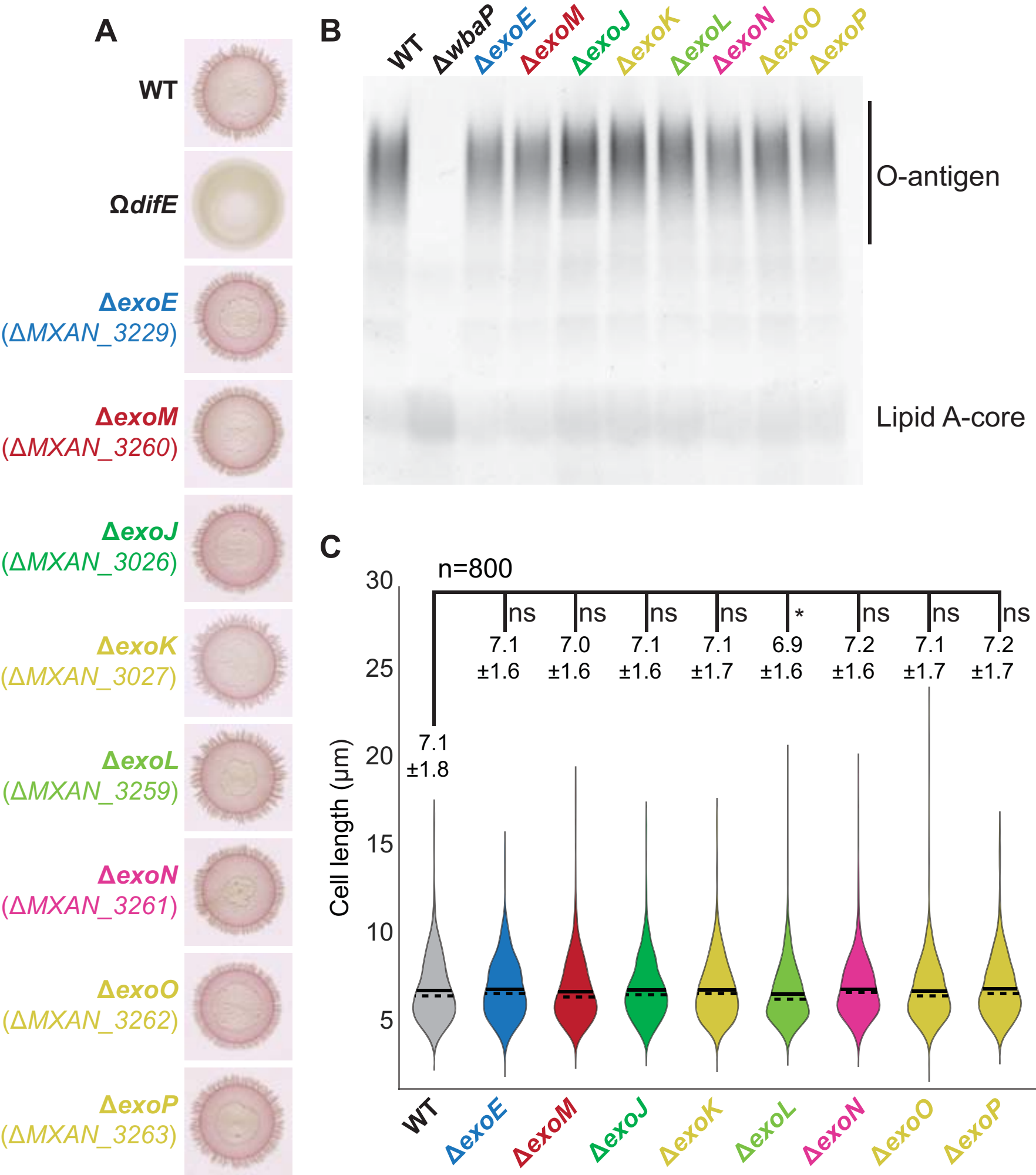
A
WT
ΩdifE
ΔexoE
(ΔMXAN_3229)
ΔexoM
(ΔMXAN_3260)
ΔexoJ
(ΔMXAN_3026)
ΔexoK
(ΔMXAN_3027)
ΔexoL
(ΔMXAN_3259)
ΔexoN
(ΔMXAN_3261)
ΔexoO
(ΔMXAN_3262)
ΔexoP
(ΔMXAN_3263)
B
WT
ΔwbaP
ΔexoE
ΔexoM
ΔexoJ
ΔexoK
ΔexoL
ΔexoN
ΔexoO
ΔexoP
O-antigen
Lipid A-core
C
n=800
ns
ns
ns
ns
*
ns
ns
ns
7.1 ±1.8
7.1 ±1.6
7.0 ±1.6
7.1 ±1.6
7.1 ±1.7
6.9 ±1.6
7.2 ±1.6
7.1 ±1.7
7.2 ±1.7
Cell length (μm)
30
25
20
15
10
5
WT
ΔexoE
ΔexoM
ΔexoJ
ΔexoK
ΔexoL
ΔexoN
ΔexoO
ΔexoP

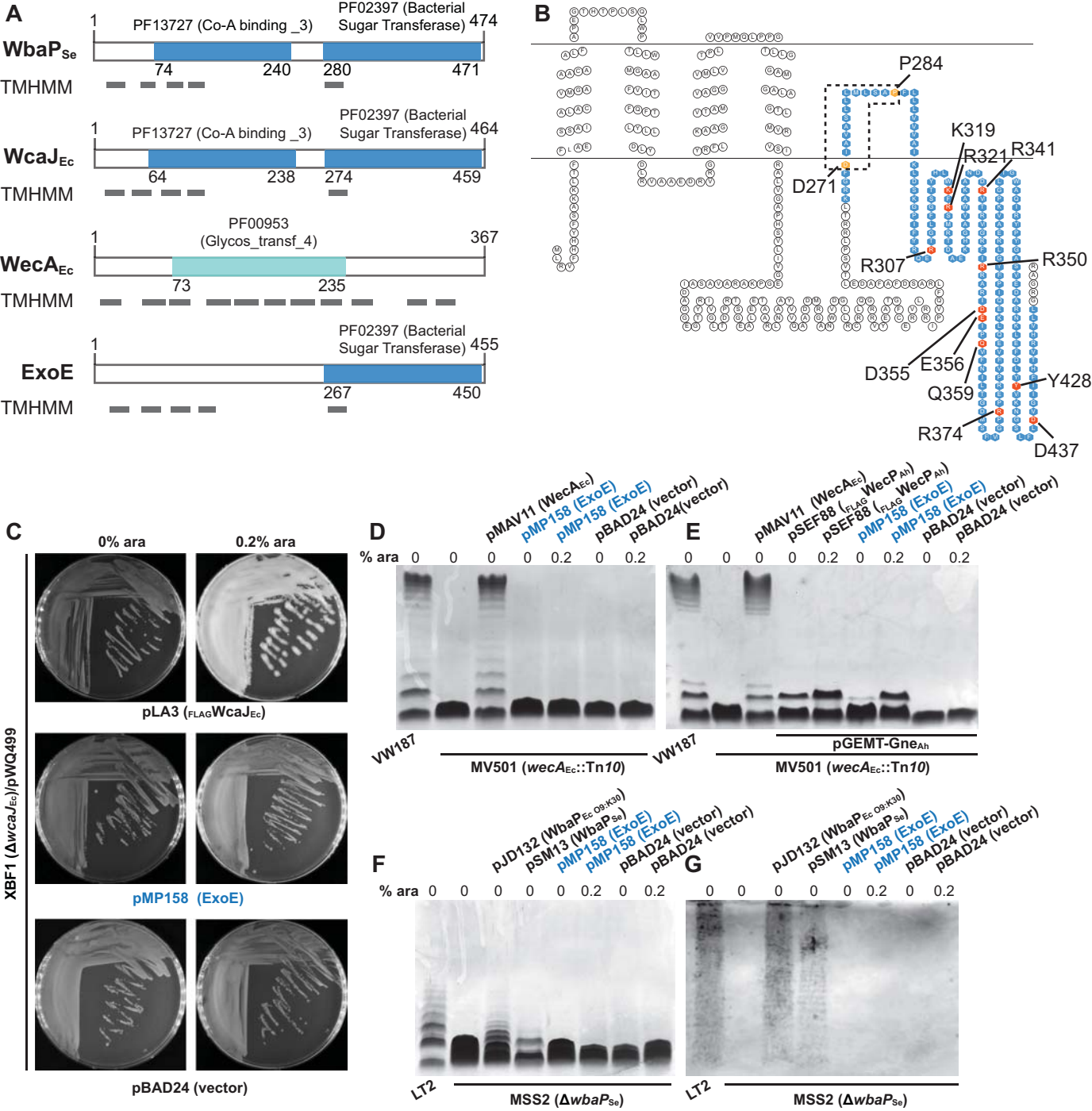
A
WbaP$_{Se}$
PF13727 (Co-A binding _3)
PF02397 (Bacterial Sugar Transferase)
1
474
74
240
280
471
TMHMM
WcaJ$_{Ec}$
464
64
238
274
459
WecA$_{Ec}$
PF00953 (Glycos_transf_4)
367
73
235
ExoE
455
267
450
B
P284
K319
R321
R341
D271
R307
R350
D355
E356
Q359
Y428
R374
D437
C
0% ara
0.2% ara
pLA3 ($_{FLAG}$WcaJ$_{Ec}$)
pMP158 (ExoE)
pBAD24 (vector)
XBF1 (ΔwcaJ$_{Ec}$)/pWQ499
D
% ara
pMAV11 (WecA$_{Ec}$)
pMP158 (ExoE)
pBAD24 (vector)
VW187
MV501 (wecA$_{Ec}$::Tn10)
E
pSEF88 ($_{FLAG}$WecP$_{Ah}$)
pGEMT-Gne$_{Ah}$
F
pJD132 (WbaP$_{Ec\ O9:K30}$)
pSM13 (WbaP$_{Se}$)
LT2
MSS2 (ΔwbaP$_{Se}$)
G

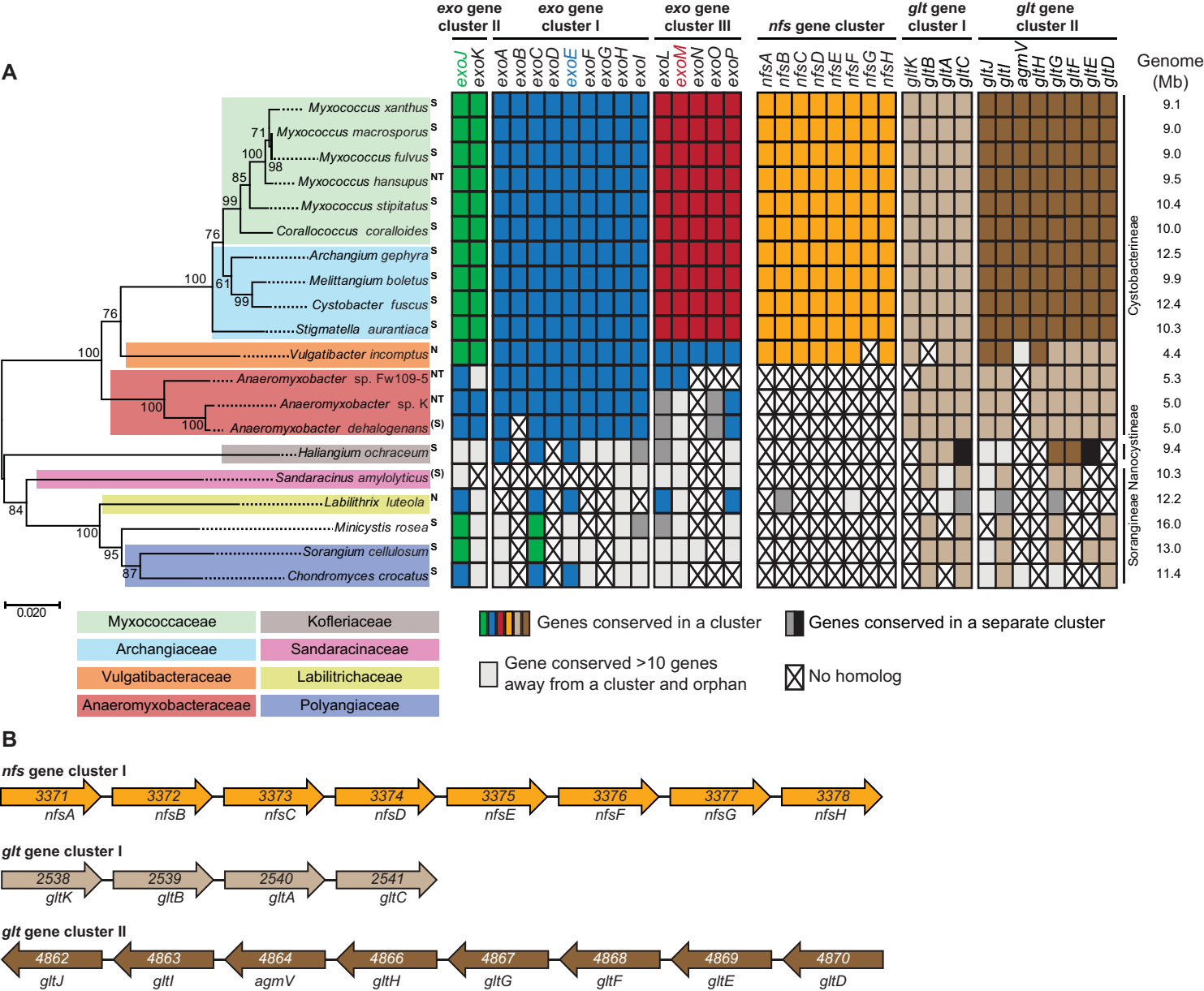
A
exo gene cluster II
exo gene cluster I
exo gene cluster III
nfs gene cluster
glt gene cluster I
glt gene cluster II
exoJ exoK exoA exoB exoC exoD exoE exoF exoG exoH exoI exoL exoM exoN exoO exoP nfsA nfsB nfsC nfsD nfsE nfsF nfsG nfsH gltK gltB gltA gltC gltJ gltI agmV gltH gltG gltF gltE gltD
Genome (Mb)
Myxococcus xanthus S 9.1
Myxococcus macrosporus S 9.0
Myxococcus fulvus S 9.0
Myxococcus hansupus NT 9.5
Myxococcus stipitatus S 10.4
Corallococcus coralloides S 10.0
Archangium gephyra S 12.5
Melittangium boletus S 9.9
Cystobacter fuscus S 12.4
Stigmatella aurantiaca S 10.3
Vulgatibacter incomptus N 4.4
Anaeromyxobacter sp. Fw109-5 NT 5.3
Anaeromyxobacter sp. K NT 5.0
Anaeromyxobacter dehalogenans (S) 5.0
Haliangium ochraceum S 9.4
Sandaracinus amylolyticus (S) 10.3
Labilithrix luteola N 12.2
Minicystis rosea S 16.0
Sorangium cellulosum S 13.0
Chondromyces crocatus S 11.4
Cystobacterineae
Sorangineae Nanocystineae
0.020
Myxococcaceae
Archangiaceae
Vulgatibacteraceae
Anaeromyxobacteraceae
Kofleriaceae
Sandaracinaceae
Labilitrichaceae
Polyangiaceae
Genes conserved in a cluster
Genes conserved in a separate cluster
Gene conserved >10 genes away from a cluster and orphan
No homolog
B
nfs gene cluster I
3371 nfsA
3372 nfsB
3373 nfsC
3374 nfsD
3375 nfsE
3376 nfsF
3377 nfsG
3378 nfsH
glt gene cluster I
2538 gltK
2539 gltB
2540 gltA
2541 gltC
glt gene cluster II
4862 gltJ
4863 gltI
4864 agmV
4866 gltH
4867 gltG
4868 gltF
4869 gltE
4870 gltD

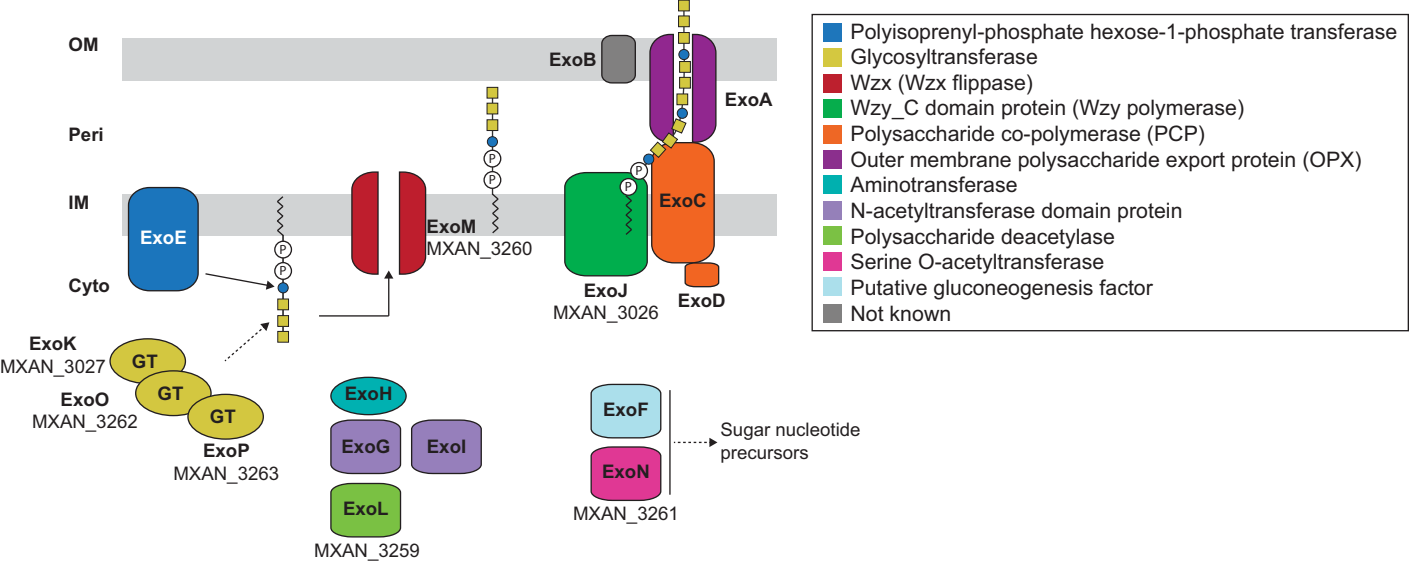
OM
Peri
IM
Cyto
ExoB
ExoA
ExoE
ExoM
MXAN_3260
ExoC
ExoJ
MXAN_3026
ExoD
ExoK
MXAN_3027
GT
GT
GT
ExoO
MXAN_3262
ExoP
MXAN_3263
ExoH
ExoG
ExoI
ExoL
MXAN_3259
ExoF
ExoN
MXAN_3261
Sugar nucleotide precursors
Polyisoprenyl-phosphate hexose-1-phosphate transferase
Glycosyltransferase
Wzx (Wzx flippase)
Wzy_C domain protein (Wzy polymerase)
Polysaccharide co-polymerase (PCP)
Outer membrane polysaccharide export protein (OPX)
Aminotransferase
N-acetyltransferase domain protein
Polysaccharide deacetylase
Serine O-acetyltransferase
Putative gluconeogenesis factor
Not known